SLAC-PUB-1410
(E)
April 1974

FUTURE DIRECTIONS IN BARYON SPECTROSCOPY*

J. A. J. Matthews
Stanford Linear Accelerator Center
Stanford University, Stanford, Calif. 94305

ABSTRACT

Recent developments in the analysis of low energy $\pi N \to \pi\pi N$ data and in the search for strangeness + 1 (Z^*) resonances are used to motivate new directions for experiments in baryon spectroscopy.

*Work supported by the U. S. Atomic Energy Commission.

(Invited paper presented at the Symposium on Production of Heavy Excited Hadrons, Argonne National Laboratory, March 8, 1974.)

I. Introduction

Baryon spectroscopy provides on one hand the well understood low mass nucleon resonance region, yet on the other the essentially unknown territory of Ξ^*, Ω^* and Z^* resonances.[1] Interesting future directions thus range from sophisticated studies of the interaction of excited nucleons to simple resonance searches.

To introduce and motivate several future directions for baryon spectroscopy, I will initially review two new results. Firstly, the three body analysis of $\pi N \rightarrow \pi\pi N$ scattering by LBL-SLAC.[2] This analysis, coupled with elastic phase shift results, provides a detailed understanding of nonstrange baryon resonances up to ~ 1.8 GeV. These baryon formation experiment results then provide a laboratory in which to study production reactions. Secondly, there has recently been some new input into the question of positive strangeness (Z^*) baryon resonances.[3-5] Such states are inconsistent with the simple three quark model for baryons. These results suggest that searches for other "exotic" states should be initiated in several channels, and in particular for resonances in unique charge states. Interesting possibilities include charge -2 Σ and Ξ resonances.

The plan for the talk is as follows. "New results" are discussed in sect. II, followed by the presentation of "new directions" for baryon spectroscopy in sect. III. The importance of searches for exotics, the production of resonances in baryon exchange reactions, the use of hyperon beams, and forward production reactions are reviewed. Finally, a summary is provided in sect. IV.

II. New Results

a) Three Body Analyses: $\pi N \to \pi\pi N$

(a.1) Experimental motivation and results

Although most phase shift analyses in baryon spectroscopy utilize only two body data, two body channels drop rapidly in importance once the energy exceeds three body threshold. This is seen to be the case for the K^-p cross sections[6] shown in fig. 1. Although the K^-p elastic cross section dominates any other single channel in the energy region considered, it is not larger than the sum of the inelastic channels. The information obtained from phase shift analyses can thus be substantially increased by including data from inelastic channels. In particular, analyses of inelastic channels:

(a) provide signs and magnitudes (partial widths) for resonance couplings into different channels,

(b) allow all decay channels to be discussed simultaneously, for example using K matrix techniques.[2]

Three body partial wave analyses have typically taken two forms. In the first, a mass selection is made in the 3-body Dalitz plot to select a dominant quasi-two body decay mode.[7,8] Since this technique does not exploit the interferences between different "quasi-two body" final states in the Dalitz plot, it suffers from the same "Minami" ambiguity difficulties as elastic analyses. The second approach is referred to as the isobar model.[2]

In the isobar model the three final state particles are decomposed into three quasi-two body amplitudes diagramatically represented by fig. 2(c). The state of spin j is parametrized with a final state enhancement factor (Breit Wigner or experimental two body phase shifts) characteristic of the two body interaction involved. The data are then fitted over the entire 3-body Dalitz plot.

To denote the different possible quasi-two body partial waves a slight modification of the usual nomenclature for baryon resonances is employed. Thus, a state of spin parity, J^P, and isospin, I, is written:

Elastic Formalism		3-body Formalism	
ℓ (2I) (2J)		ℓ L (2I) (2J)	
Examples: $\pi N \to \pi N$		$\pi N \to \pi\pi N$	
$I = \frac{1}{2}$, $J^P = \frac{1}{2}^-$	S11	SS11 SP11	(ρN decay) (ϵN decay)
$I = \frac{1}{2}$, $J^P = \frac{1}{2}^+$	P11	PP11 PS11	($\pi\Delta$ decay) (ϵN decay)

The relative angular momentum in initial and final channels, ℓ and L, are as shown in fig. 2(c).

The LBL-SLAC analysis(2) of $\pi N \to \pi\pi N$ involves several thousand events, at each of eighteen energies between 1.31 GeV and 1.97 GeV. Data in the three channels

$$\pi^- p \rightarrow \pi^+ \pi^- n$$
$$\pi^- p \rightarrow \pi^- \pi^0 p \qquad (1)$$
$$\pi^+ p \rightarrow \pi^+ \pi^0 p$$

are simultaneously fitted using the resonance decay parameterizations:

$$\pi N \rightarrow \pi\Delta$$
$$\rightarrow \rho N \qquad (2)$$
$$\rightarrow \epsilon N$$

Independent partial wave amplitude solutions are obtained at each energy, and in both isospin $I = \frac{1}{2}$ and $I = \frac{3}{2}$ channels. Finally, two continuous solutions (A and B) have been found smoothly connecting the independent solutions through the entire energy region.

The results for the $I = \frac{1}{2}$ N^* phase shifts are shown in fig. 3. Phase shifts within the heavily outlined rectangles are for one partial wave; each subrectangle represents one or more possible decay channels from eqn. 2. As in elastic analyses, resonances are defined by counter-clockwise loops in the Argand plot. However one obtains a bonus from inelastic analyses, obtaining the relative signs of the resonance couplings by observing whether the resonant loop initiates its motion in a positive (upward) or in a negative (downward) sense.

The magnitude of a given partial wave is represented by the distance of the solution from the center of the Argand plot. Typical examples are shown on the right of fig. 4 where the amplitudes are plotted as a function of energy.

The cross section for the inelastic channels $\pi N \rightarrow \pi\pi N$ can also be compared to the inelastic cross sections predicted by elastic phase shift analyses. This is shown for the P11 wave in the top of fig. 4; good agreement is generally observed throughout the energy region studied.

(a.2) Comparisons with SU(6)

The signs of the couplings(9) for nucleon resonances decaying into $\pi\Delta$ are shown in fig. 5. The "clocks" show the $SU(6)_W$ predictions for the coupling signs,(9) up being positive, and down negative. The LBL-SLAC data,(2) solution B, are given by the "X"'s in the figure. Agreement with the theoretical predictions is observed for all resonance couplings, excepting the N*(1690) and N*(1750). Considering that there are both experimental and theoretical uncertainties,(9) the agreement is quite remarkable.

The present status of the classification of baryon resonances in the SU(6) quark model(9) is shown in fig. 6. Blank spaces in fig. 6(b) represent missing states. However, even extensive additional experimental effort in the $\gtrsim$ 2 GeV mass region (in traditional channels) will provide few constraints on these quark models, and is probably unwarranted. Of more interest are searchs directed towards less well measured decay modes: $N^* \rightarrow N\omega$, ΛK^*, etc. These channels may become important for high mass high spin resonances.

A second interesting approach is to search for states either outside the simple quark model predictions (see sects. IIb and III on exotics), or for resonances in yet unobserved representations of SU(6).

In particular, the simple quark model yields the SU(6) classifications:[10]

$$
\begin{aligned}
&\text{Baryons} \qquad qqq = \underset{\sim}{56} + \underset{\sim}{70} + \underset{\sim}{70} + \underset{\sim}{20} \\
&\text{Mesons} \qquad q\bar{q} = \underset{\sim}{35} + \underset{\sim}{1}
\end{aligned}
\tag{3}
$$

which can be decomposed into the more familiar SU(3), SU(2) representations:

$$
\begin{aligned}
\underset{\sim}{56} &= \underset{\sim}{10}^{4} + \underset{\sim}{8}^{2} \\
\underset{\sim}{70} &= \underset{\sim}{10}^{2} + \underset{\sim}{8}^{2} + \underset{\sim}{1}^{2} + \underset{\sim}{8}^{4} \\
\underset{\sim}{20} &= \underset{\sim}{8}^{2} + \underset{\sim}{1}^{4}
\end{aligned}
\tag{4}
$$

using the notation $\underset{\sim}{SU(3)}^{2S+1}$, and S is the net spin of the three quarks in an L-S coupling scheme. Since experimental beams (mesons) and targets (baryons) fall in the $\underset{\sim}{35}$ and $\underset{\sim}{56}$ representations respectively, formation experiments will only result in excited baryons in the group representations:

$$\underset{\sim}{35} \times \underset{\sim}{56} = \underset{\sim}{56} + \underset{\sim}{70} + \cdots \text{ (no 20's)} \tag{5}$$

In particular, states in $\underset{\sim}{20}$ representations do not result from formation experiments. However, such resonances may be formed in the decay chain of higher mass $\underset{\sim}{70}$'s,[11] or may be produced in backward (baryon exchange) reactions:

$$\underset{\sim}{35} \times \underset{\sim}{70} = \underset{\sim}{20} + \underset{\sim}{56} + \underset{\sim}{70} + \cdots . \tag{6}$$

At moderate laboratory energies, ~ 6 Gev/c, baryon exchange cross sections are still large enough that backward production reactions may provide the most attractive means of searching for baryons in $\underset{\sim}{20}$ representations.

b) The Z* question

(b.1) Overview

In contrast to the extensive documentation of strangeness ≤ 0 baryons, the existence of strangeness + 1 baryon resonances is still unclear. Analyses of K^+p data suggest that the P13 wave, $Z^*_{I=1}$, may resonate[12] at a mass ~ 1.9 GeV. Unfortunately the large inelasticity of this partial wave makes the interpretation difficult. The existence of this state is considered doubtful.[8,13,14] However the results in the isospin zero channel[3] are more promising, and are consistent with a resonant P01 wave, $Z^*_{I=0}$, at a mass ~ 1.74 GeV.

The existence of one or both of these states has interesting implications for the simple quark model, and for the normal SU(3) classification schemes. In particular such states cannot be formed from three quarks but require, at least, the structure $qqqq\bar{q}$. The resulting simplest SU(3) representations containing these states are the $\underset{\sim}{27}$ and $\underset{\sim}{\overline{10}}$ representations for $Z^*_{I=1}$ and $Z^*_{I=0}$ respectively. This is shown in fig. 7, along with the other unique baryon resonances which would cohabit in these SU(3) representations. Of particular interest is the possibility of charge -2 Σ, Ξ and Ω resonances. These topics will be discussed in more detail in sect. III.

(b.2) $Z^*_{I=1}$

Phase shift analyses of K^+p elastic and inelastic data have failed to find clear evidence of isospin one resonances. A typical set of phase shift solutions[14] are shown in fig. 8. Although the P_3 wave has some characteristics of a resonance (counterclockwise movement in the Argand diagram), the speed plots of the phase[14] indicate no obvious resonant behavior. Rather, the P_3 wave appears merely to respond to the rapidly opening KN $\rightarrow$ KπN channel.[15] This is shown in fig. 9 where the KN reaction is observed to be substantially inelastic by a momentum of $\sim$ 1.5 GeV/c (corresponding to $\sim$ 2GeV in Kp mass).

Detailed studies of the Kp elastic data confirm that substantial changes also occur in the shape of the elastic differential cross section near KπN threshold.[16] This is shown in fig. 10 where the dramatic rise in both the slope and forward cross section of the elastic data is precisely correlated with KN $\rightarrow$ KπN threshold. Thus, the close relationship between inelastic and elastic channels suggests that a three body analyses may well provide invaluable insights into the questions of Z* resonances in the $\sim$2 Gev mass region.

(b.3) $Z^*_{I=0}$

A rather involved multichannel procedure is involved in obtaining isospin zero KN phase shifts. This results from the data being a mixture of I = 0 and I = 1 channels. For example, typical analyses use data on the reactions:

$$A_{K^+n\rightarrow K^+n} = \frac{1}{2}\left(Z_{I=1} + Z_{I=0}\right)$$
$$A_{K^+n\rightarrow K^0p} = \frac{1}{2}\left(Z_{I=1} - Z_{I=0}\right) \qquad (7)$$

Thus a K^+p phase shift analysis is simultaneously involved in extracting $Z^*_{I=0}$ amplitudes.

The results of the recent BGRT analysis[3] are shown in fig. 11. Three classes of acceptable solutions emerge, denoted A, C, and D in the figure. The essential difference between these solutions resides in the $S_{1/2}$ and $P_{1/2}$ partial waves. Of the different solutions, the $P_{1/2}$ wave in solution D most nearly characterizes a resonant partial wave. A parameterization of this solution with a Breit Wigner yields:[3]

$$M_{Z^*_{I=0}} \sim 1740 \text{ Mev}$$

$$\Gamma_{Z^*_{I=0}} \sim 300 \text{ MeV}$$

(inelasticity) $$X_{Z^*_{I=0}} \sim 0.85$$

To determine whether solution D is in fact the correct solution, comparisons of the ambiguous phase shift solutions can be made to data not included in the original analysis. One such comparison[3] is shown in fig. 12a. Although the uncertainties in the $K^+n \rightarrow K^0p$ polarization are large, solutions C and D are favored over solution A.

Recently, a second comparison[4] has been made using data in the reaction $K^0_Lp \rightarrow K^0_Sp$. In this reaction three amplitudes contribute:

$$A_{K^0_Lp\rightarrow K^0_Sp} = \frac{1}{4}\left(Z_0 + Z_1 - 2Y_1\right) \tag{8}$$

where the additional amplitude, Y_1, is the isospin one, strangeness -1 scattering amplitude. The strong Σ (1765) resonance (in the mass interval of interest for the $Z^*_{I=0}$ analysis) interfers with the strangeness +1 amplitudes to provide substantial differences in the $K^0_Lp \rightarrow K^0_Sp$ cross section predictions, as shown in fig. 12b. In conclusion the C and D phase shift solutions are again favored over solution A by this comparison.

Thus, although the existence of a $Z^*_{I=0}$ resonance is not proved by these analyses, the favored partial wave solutions do contain an interesting resonance candidate in the $P_{1/2}$ partial wave. As with the K^+p channel, the nearness of the possible $Z^*_{I=0}$ to the threshold for $KN \rightarrow K\pi N$,(3) see fig. 13, again suggests that an analysis of the three body channels is of particular relevance to our understanding of Z^* resonances.

III. New Directions.

a) Ξ^* and Ω^* resonances

The impossibility of studying Ξ^* or Ω^* resonances in direct channel formation experiments has substantially retarded our understanding of these states in comparison to our knowledge of their strangeness 0 and -1 brothers. Little data exists for any of the excited Ξ^* states; no observation has been made of excited Ω^* states.

Typical statistics for Ξ^* experiments[17,18] are shown in fig. 14; thus even relatively simple experiments are of interest. Possible priorities in the search for Ξ^* and Ω^* resonances include:

(a) a measurement of the masses and widths,

(b) a determination of the decay channel partial widths, and

(c) only lastly, a spin-parity analysis of the resonances.

Unless the data prove totally unexpected (no Ω^* resonances, or unusual decay partial widths for example) extensive analyses are not warranted. This is particularly true for Ξ^* resonances which, appearing in both $\underset{\sim}{8}$ and $\underset{\sim}{10}$ SU(3) representations, will correspondingly provide few constraints on theoretical models.

Unfortunately Ξ production cross sections are small,[19] as shown in fig. 15. At lower energies, $\lesssim 6$ GeV/c, the production of Ξ^*'s in backward (baryon exchange) reactions may yield a sample of events relatively rich in Ξ's. This is illustrated in fig. 16 where the backward cross sections for $K^-p \to \Xi^{*0}(1530)K^0$ [18] and $\pi^-p \to \Lambda^0 K^0$ [20] are compared.

Both reactions require Σ exchange in the u channel, and the observed cross sections are indeed similar.

Simultaneous with the study for backward Ξ^*'s, at least as much effort should go into searches for exotic Ξ^* resonances! Of particular interest is the question of Ξ^{--} states,[21] see fig. 7, which would be suggested by the existence of either $Z^*_{I=0}$ or $Z^*_{I=1}$ resonances. Typical existing results in this channel, shown in fig. 17, do not yet have sufficient statistics to allow a meaningful study to be made. Interestingly, Ξ^{--} states may be produced with cross sections similar to non-exotic Ξ resonances, as suggested by the backward reactions:

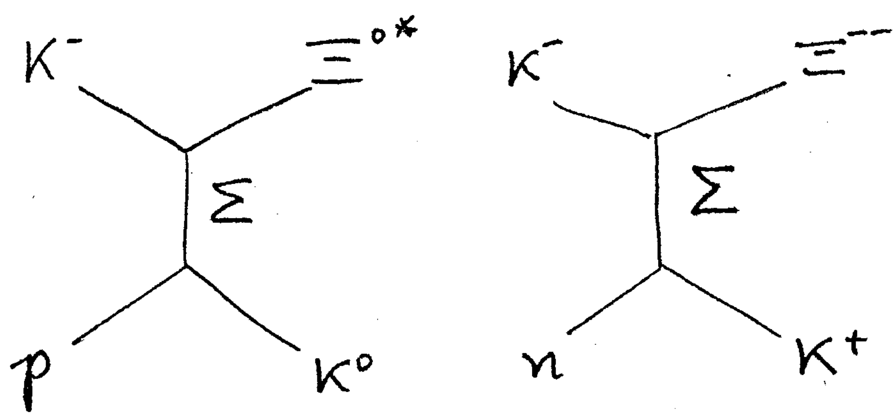

(normal) (exotic)

A possible objection to this model is discussed in sect. III(b).

At higher beam energies Ξ's are produced predominantly near $x = 0$,[22] and as a result are potentially more difficult to select in an experimental trigger. In this case the solution may be to generate a hyperon beam. An example of the particle fluxes from the CERN hyperon beam[23] is shown in fig. 18. Although data rates using these beams may be low, they provide probably the only mechanism to study Ω^*'s, and an alternate means of studing Ξ^* resonances.

b) Exotics

As introduced in sect. IIb, exotic baryons are (nominally) states that cannot be formed from three quarks. This leaves rather a wide scope for our imagination; for recent discussions see for example Faiman, Goldhaber and Zarmi,[24] or Freund.[25] Possibly the simplest scheme for exotics would include only those states in the $\underset{\sim}{27}$ and $\underset{\sim}{\overline{10}}$ representations shown in fig. 7 and related to the Z* resonances described in sect. IIb.

On general grounds searches for exotics should:[24]

(a) choose manifestly <u>exotic</u> <u>charge</u> quantum numbers, for example, $\underset{\sim}{27}$, $\underset{\sim}{\overline{10}}$ and $\underset{\sim}{35}$ representations have many highly charged states;

(b) pick "allowed" production and decay channels, for example, Faiman, Goldhaber and Zarmi[24] suggest using "connected quark diagrams";

(c) select channels with a small number of decay particles, and/or particles that are identifiable (highly charged exotics help here).

For reference, typical masses for exotic baryons are expected to be $\gtrsim 2$ GeV, however the possible $Z^*_{I=0}$ state at a mass of ~1.74 GeV may indicate that exotics will appear at somewhat lower masses than predicted.

Unfortunately, the observation of exotics may well depend on the experiment being well coupled to the physics of the production mechanism. Already we know that formation experiments, for example $K^+N \rightarrow Z^*$'s, do not yield blatant resonant exhancements. Perhaps this will be true of the majority of production reactions, as is in fact suggested by quark diagram models. To understand what this implies, consider the reactions $\pi^+ p \to K^{*-} Z^{+++}$(24) and $K^- n \to \Xi^{--} K^+$ whose "allowed" quark line diagrams are shown in fig. 19. Inspection of the t and u channel exchanges in these diagrams indicates that exotic meson and baryon exchange is required for Z^{+++} and Ξ^{--} production respectively. Such exotic exchanges would be related to low lying Reggeon trajectories (assuming exotics are more massive than nonexotics of the same spin), and would result in very small cross sections for these reactions. In many cases this is only brought out by quark model arguments; naive predictions in sect. IIIa for $K^- n \to \Xi^{--} K^+$ and the nonexotic reaction $K^- p \to \Xi^0 K^0$ suggest approximate equality for these cross sections! Thus exotics may well elude discovery for many more years.

c) Forward Production Reactions

As an introduction to baryon spectroscopy in forward production reactions, it is instructive to make a short comparison of formation vs. production experiments.

Formation	Production
Advantages	**Advantages**
- high statistics	- only means of studying mesons
- variable experimental conditions; for example energy, isospin, strangeness	- may allow certain states of spin-parity to be preferentially produced, for example $p_f = p_i(-1)^{\Delta J}$ for diffractive production
- particles on the mass shell	- unique features in baryon exchange reactions, discussed in sect. IIa, IIIa.
Disadvantages	**Disadvantages**
- limited beams or targets, for example, no meson targets	- final state interactions, or overlapping kinematics may cloud the physics interpretation
- limited physical acceptance of experimental apparatus	- particles off the mass shell

From this comparison, we wish to emphasize that meson resonances are only studied in production experiments. This suggests that the relatively well understood spectroscopy of nucleon resonances should be used as a "test laboratory" for studying production processes:

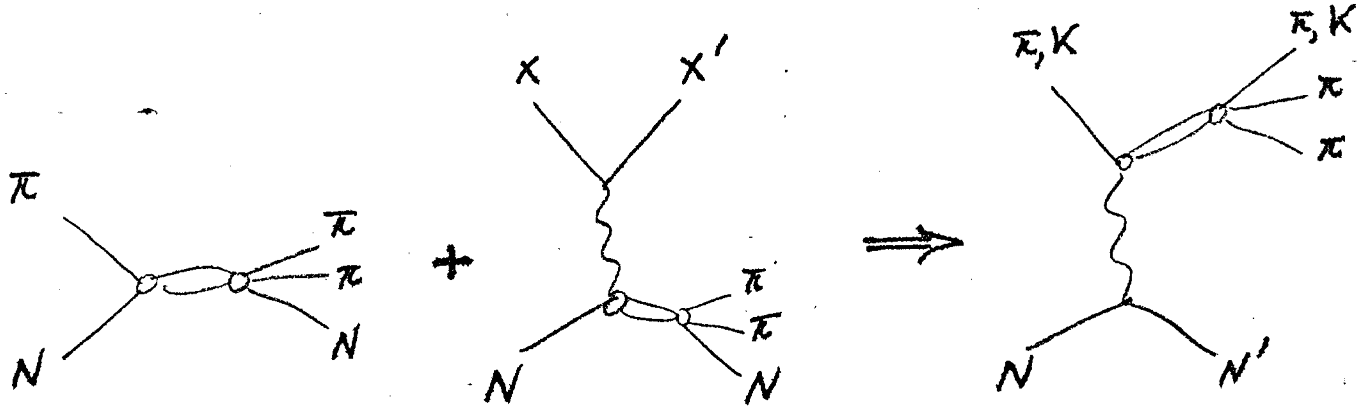

(known) + (test laboratory) ===> (mesons unravelled)

Several interesting questions on production reactions can be asked immediately.

(a) What is the relation of the baryon spectrum produced diffractively (Pomeron exchange) or non-diffractively (for example by charge exchange) with the results of formation experiments? One difficulty with this analysis results from the differences in the momentum transfer dependences of the differential cross sections for various baryon resonances. The striking effect of making several momentum transfer cuts on the data[26] is shown in fig. 20.

(b) What is the importance of final state interactions on the produced resonance spectrum? Variation of experimental conditions such as beam energy, or the type of beam particle,[26] as shown in fig. 21, may elucidate this issue. Studies of the baryon spectrum for different decay channels,[26] as illustrated in fig. 22, is also of interest.

Finally, polarized targets (or beams) may be a useful tool in understanding production dynamics. One example is the amusing experiment suggested by Berger and Fox[27] to test whether diffractively produced states interact like a single particle, or like a "two body" system following the Deck model predictions.

IV. Summary.

The advances in our understanding of the πN spectrum and in particular the recent progress in the three body analysis $\pi N \to \pi\pi N$ suggest:

(a) that similar (3 body) analysis be done in Y^* and Z^* channels,

and (b) that baryon production data is essential in elucidating meson production results.

In the area of particle searches, the success of the quark model prediction for the πN system invites experimental testing of the basic quark model assumptions:

(a) searches for resonances in $\underset{\sim}{20}$ representations, and

(b) extension of exotic searches from simple Z^*'s in formation reactions, to a wide variety of states in production reactions (e.g., Ξ^{--}, Z^{+++}, ...).

Finally, completeness demands particle survey experiments for Ξ and Ω resonances probably best done using hyperon beams.

V. Acknowledgments.

I would like to thank R. Cashmore, F. Gilman, T. Lasinski and D. Leith for invaluable discussions on baryon spectroscopy. I would also like to thank D. Leith for his support and interest.

References

1) For useful reviews see for example:

Proceedings of Purdue Conference on Baryon Spectroscopy, Ed. E. C. Fowler, Purdue Univ. Press (1973);

J. L. Rosner, AIP Conference Proceedings #14, Eds. H. H. Bingham, M. Davier, G.R. Lynch, AIP Press (1973);

J. L. Rosner, "The Classification and Decays of Resonant Particles", SLAC-PUB-1391 (1974);

N. P. Samios, M. Goldberg, B. T. Meadows, "Hadrons and SU(3): A Critical Review", BNL 17851 (1973);

Proceedings of the Conference on Hyperon Resonances, Ed. E. C. Fowler, Moore Publishing Co. (1970);

A. Barbaro-Galtieri, "Selected Topics in Baryon Resonances", LBL-555 (1972).

2) D. J. Herndon, R. Longacre, L. R. Miller, A. H. Rosenfeld, G. Smadja, P. Soding, R. J. Cashmore, D.W.G.S. Leith, "A Partial Wave Analysis of the Reaction $\pi N \to \pi\pi N$ in the C. M. Energy Range 1300-2000 MeV", SLAC-PUB-1108 (1972);

R. J. Cashmore, Proceedings of Purdue Conference on Baryon Spectroscopy, Ed. E. C. Fowler, Purdue Univ. Press (1973);
R. J. Cashmore, "Amplitude Analysis in Three Body Final States", SLAC-PUB-1316 (1973).

3) B.G.R.T. Collaboration, "Phase Shift Analysis of $K^+N \to KN$ Scattering in the I = 0 State Up to 1.5 GeV/c", CERN preprint (1973).

4) G. W. London, "The Reaction $K_L^0 p \to K_S^0 p$ and the Possible Existence of a Z_0^* Resonance", BNL preprint NG-267 (1973).

5) A. S. Carroll, T. F. Kycia, K. K. Li, D. N. Michael, P. M. Mockett, D.C. Rahn, R. Rubinstein, Phys. Lett. 45B, 531 (1973).

6) P. J. Litchfield, Proceedings of RHEL Meeting on K-Meson Physics Below 5 GeV/c, Ed. G. C. Oades, Rutherford Publ. RHEL/R 245 (1972).

7) A. D. Brody, A. Kernan, Phys. Rev. 182, 1785 (1969);
A. D. Brody, R. J. Cashmore, A. Kernan, D.W.G.S. Leith, B.G. Levi, B. C. Shen, D. J. Herndon, L. R. Price, A. H. Rosenfeld, P. Soding, Phys. Lett. 34B, 665 (1971);

T. S. Mast, M. Alston-Garnjost, R.O. Bangerter, A. Barbaro-Galtieri, F. T. Solmitz, R. D. Tripp, Phys. Rev. Lett. 28, 1220 (1972);

8) B.G.R.T. Collaboration, Nucl. Phys. B38, 365 (1972);

R. W. Bland, M.G. Bowler, J.L. Brown, J.A. Kadyk, G. Goldhaber, S. Goldhaber, V.H. Seeger, G.H. Trilling, Nucl. Phys. B13, 595 (1969).

9) J. L. Rosner, see ref. 1.

10) See for example: S. Meshkov, Proceedings of the conference on Hyperon Resonances, Ed. E. C. Fowler, Moore Publishing Co. (1970).

11) D. Yaffe, V. Chaloupka, A. Ferrando, M. Losty, L. Montanet, E. Paul, A. Zieminski, Proceedings of the Purdue Conference on Bayon Spectoscopy, Ed. E. C. Fowler, Purdue Univ. Press (1973).

12) M. G. Albrow, S. Anderson, B. Bošnjakovic, C. Daum, F. C. Erné, Y. Kimura, J. P. Lagnaux, J. C. Sens, F. Udo, F. Wagner, Nucl. Phys. B30, 273 (1971);

B.G.R.T. Collaboration, Nucl. Phys. B20, 301 (1970).

13) C. Lovelace, F. Wagner, Nucl. Phys. B28, 141 (1971).

14) J. D. Dowell, Proceedings of the Purdue Conference on Baryon Spectroscopy, Ed. E. C. Fowler, Purdue Univ. Press (1973).

15) A. A. Hirata, Proceedings of RHEL Meeting on K-Meson Physics Below 5 GeV/c, Ed. G. C. Oades, Rutherford Pub. RHEL/R 245 (1972).

16) Bristol-Rutherford-Aarhus-Southampton collab., Proceedings of the Purdue Conference on Baryon Spectroscopy, Ed. E. C. Fowler, Purdue Univ. Press (1973).

17) S. R. Borenstein, J.S. Danburg, G. R. Kalbfleisch, R. C. Strand, V. VanderBurg, J. W. Chapman, R. K. Kiang, J. Lys, Phys. Rev. D5, 1559 (1972);

18) R. T. Ross, J. L. Lloyd, D. Radojicic, Proceedings of the Purdue Conference on Baryon Spectroscopy, Ed. E. C. Fowler, Purdue Univ. Press (1973).

19) J. Badier, E. Barrelet, G. R. Charlton, I. Videau, Nucl. Phys. B37, 429 (1972).

20) G. Bellettini, Proceedings of 14th International Conference on High Energy Physics, Eds. J. Prentki and J. Steinberger, CERN (1968).

21) P. E. Schmidt, Proceedings of the Purdue Conference on Baryon Spectroscopy, Ed. E. C. Fowler, Purdue Univ. Press (1973);

D. J. Crennell, U. Karshon, K. W. Lai, J. S. O'Neall, J. M. Scarr, T. G. Schumann, Phys. Rev. D1, 847 (1970).

22) W. Barletta, M. Johnson, T. Ludlam, A. J. Slaughter, H. D. Taft, Phys. Rev. D7, 3233 (1973).

23) G. Giacomelli, Proceedings of the Amsterdam International Conference on Elementary Particles, Eds. A. Tenner and M. Veltman, North Holland (1972).

24) D. Faiman, G. Goldhaber, Y. Zarmi, Phys. Lett. 43B, 307 (1973).

25) P. G. O. Freund, Proceedings of the Purdue Conference on Baryon Spectoscopy, Ed. E. C. Fowler, Purdue Univ. Press (1973).

26) D. R. O. Morrison, "Review of Quasi Two-Body Reactions", CERN/D.Ph II/Phys 71-10 (1971).

27) G. Fox, Proceedings of the 2nd International Conference on Polarized Targets, Ed. G. Shaprio, LBL Publication LBL-500 (1971).

Figures

1) Observable cross sections for low energy K^-p scattering from ref. 6.

2) Comparison of a) formation and b) production experiments. The analysis of three body states in the isobar model, ref. 2, is depicted in c).

3) Results of the LBL-SLAC $\pi N \rightarrow \pi\pi N$ phase shift analysis, ref. 2, for $I = \frac{1}{2}$ partial waves.

4) Comparison of elastic and three body phase shifts for the P11 partial wave. The amplitudes for $\pi N \rightarrow \pi\Delta$ and $\pi N \rightarrow \epsilon N$ channels are given as a function of energy on the right of the figure. The results are from ref. 2.

5) Comparison of the signs for resonance couplings into $\pi\Delta$. The $SU(6)_W$ predictions[9] are represented by arrows, the $\pi N \rightarrow \pi\pi N$ phase shift results[2] by "X"'s.

6) Placement of baryon resonances into SU(6) quark model representations, for a) leading resonances, b) all resonances less than ~ 2 GeV. Empty rectangles correspond to presently unobserved resonances. The compilation is from ref. 9.

7) Simplest SU(3) representations containing the possible $Z^*_{I=0}$ and $Z^*_{I=1}$ resonances.

8) Two phase shift solutions (I and II) for K^+p scattering below 1.5 GeV/c.[14] The data points are shown at 100 MeV/c intervals.

9) Energy dependence of K^+p cross sections from ref. 15.

10) Differential cross section for K^+p elastic scattering[16] near three body threshold. The differential cross sections at $t = 0$, and the forward slopes are given in b) and c) respectively.

11) Argand plots showing three solutions (A, C and D) for $I = 0$ KN phase shifts from ref. 3.

12) Comparison of $I = 0$ KN phase shift solutions A, C and D to a) $K^+n \rightarrow K^0p$ polarization data,[3] and b) $K^0_Lp \rightarrow K^0_Sp$ total cross sections.[4]

13) Energy dependence of $I = 0$ KN cross sections, from ref. 3.

14) Examples of Ξ^* resonances from a) ref. 17 and b) ref. 18.

15) Cross section for Ξ^- production from ref. 19. The total cross section for $K^-p \rightarrow \Xi^-$ + anything is shown by the top curve, the lower curve is for the two body reaction $K^-p \rightarrow \Xi^-K^+$.

16) Comparison of the backward cross sections for
a) $K^-p \rightarrow \Xi^*(1530)K$, between 3.1 and 3.6 GeV/c,[18] and
b) $\pi^-p \rightarrow \Lambda^0K^0$, between 4 and 12 GeV/c.[20]

17) Typical eivdence for Ξ^{--} resonances, from ref. 21.

18) Fluxes in the CERN hyperon beam, from ref. 23.

19) Quark graphs for production of exotic baryons in the reactions $\pi^+ p \rightarrow K^{*-} Z^{+++}$ (24) and $K^- n \rightarrow \Xi^{--} K^+$.

20) Dependence of the baryon spectrum on momentum transfer observed in production experiments.(26)

21) Dependence of the baryon spectrum on beam particle observed in production experiments.(26)

22) Decomposition of the baryon spectrum in production experiments into two body and three body decay channels.(26)

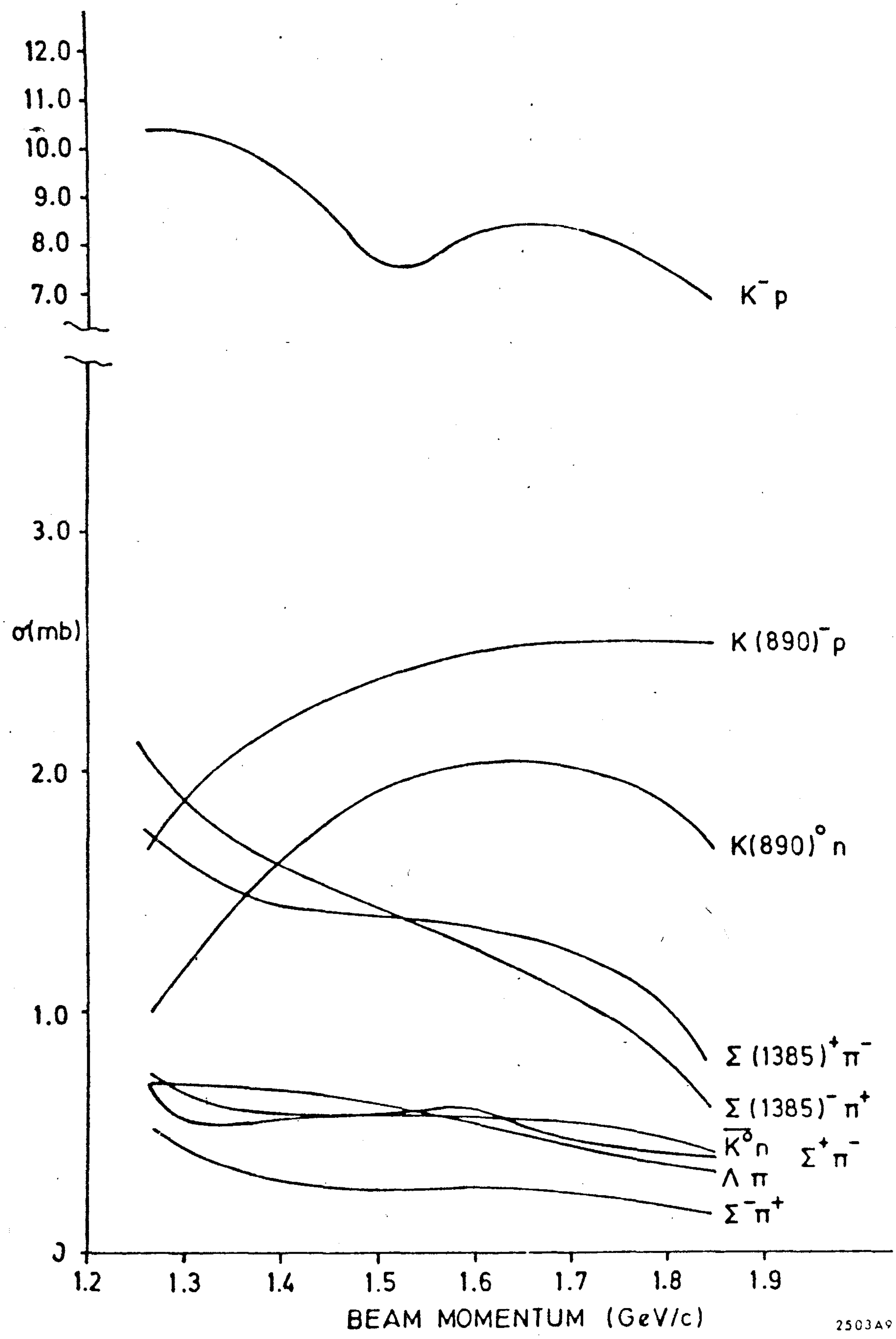
12.0
11.0
10.0
9.0
8.0
7.0
K⁻p
3.0
σ(mb)
K(890)⁻p
2.0
K(890)° n
1.0
Σ (1385)⁺π⁻
Σ (1385)⁻π⁺
K̄°n
Σ⁺π⁻
Λ π
Σ⁻π⁺
0
1.2
1.3
1.4
1.5
1.6
1.7
1.8
1.9
BEAM MOMENTUM (GeV/c)
2503A9

Fig. 1

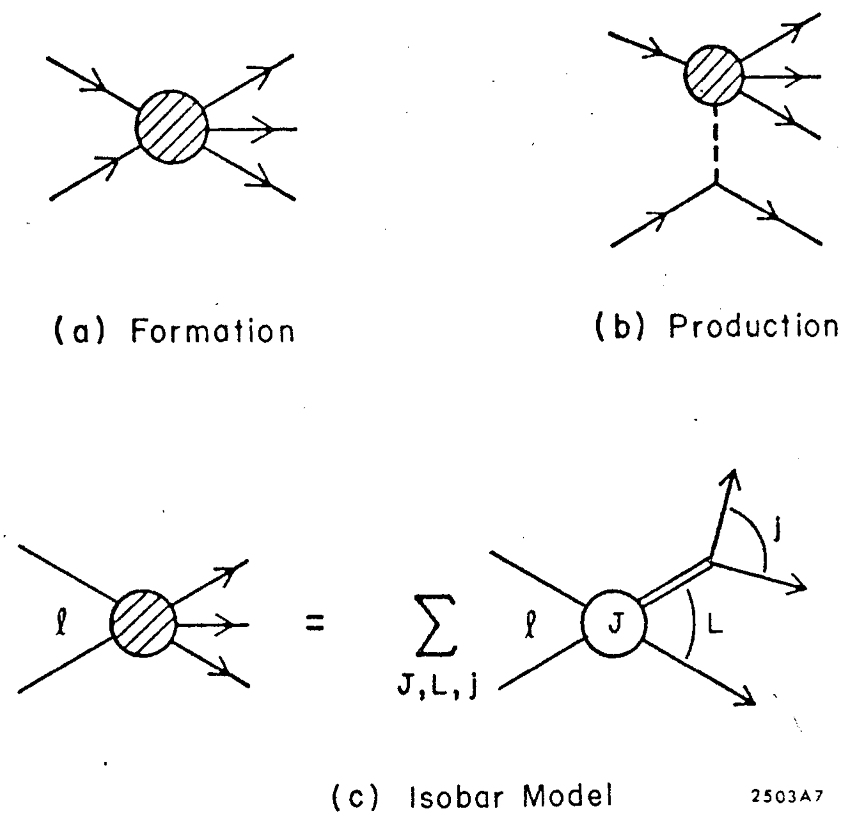

Fig. 2

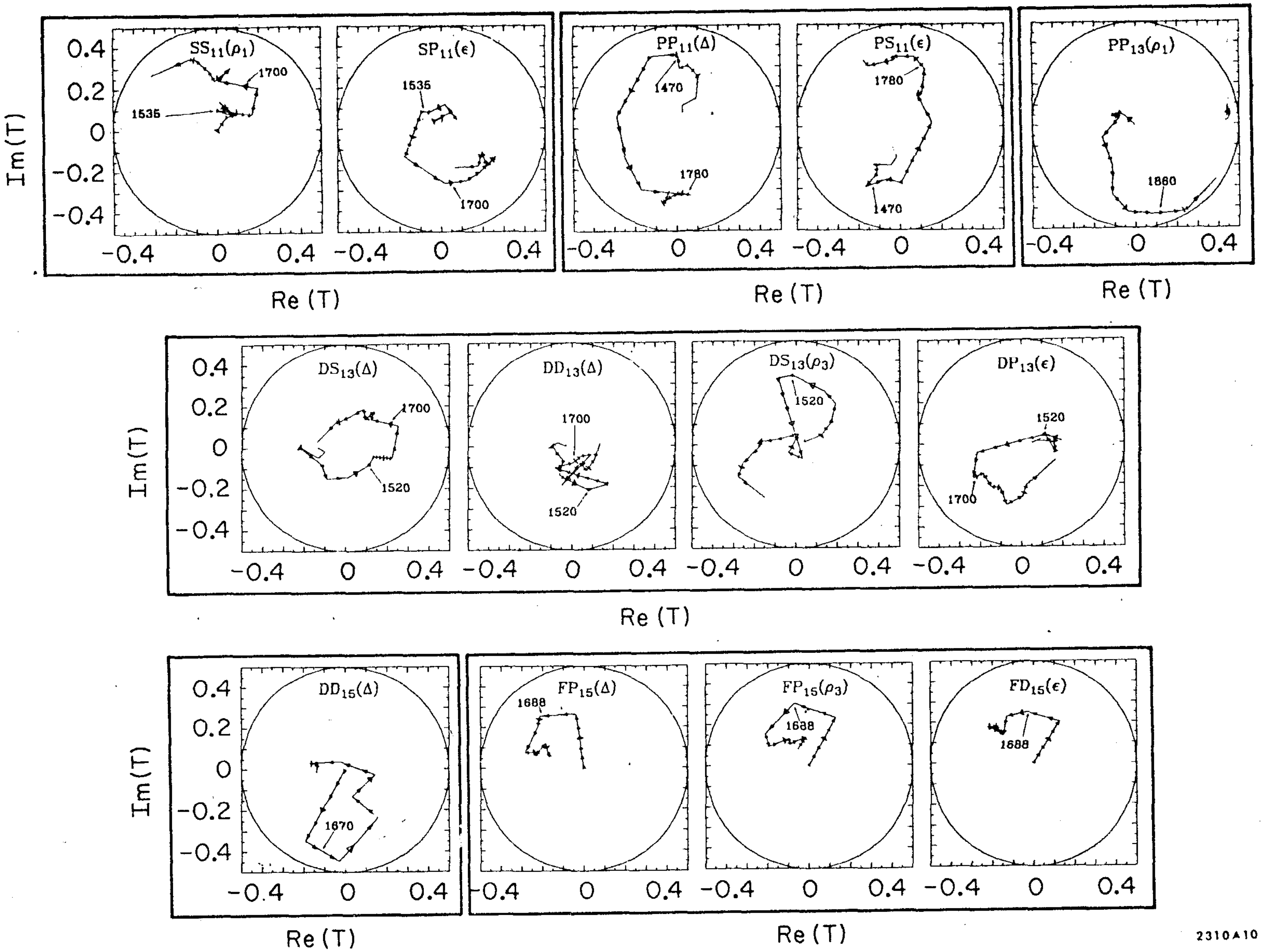
SS11(ρ1)
SP11(ε)
PP11(Δ)
PS11(ε)
PP13(ρ1)
DS13(Δ)
DD13(Δ)
DS13(ρ3)
DP13(ε)
DD15(Δ)
FP15(Δ)
FP15(ρ3)
FD15(ε)
Im(T)
Re (T)
2310A10

Fig. 3

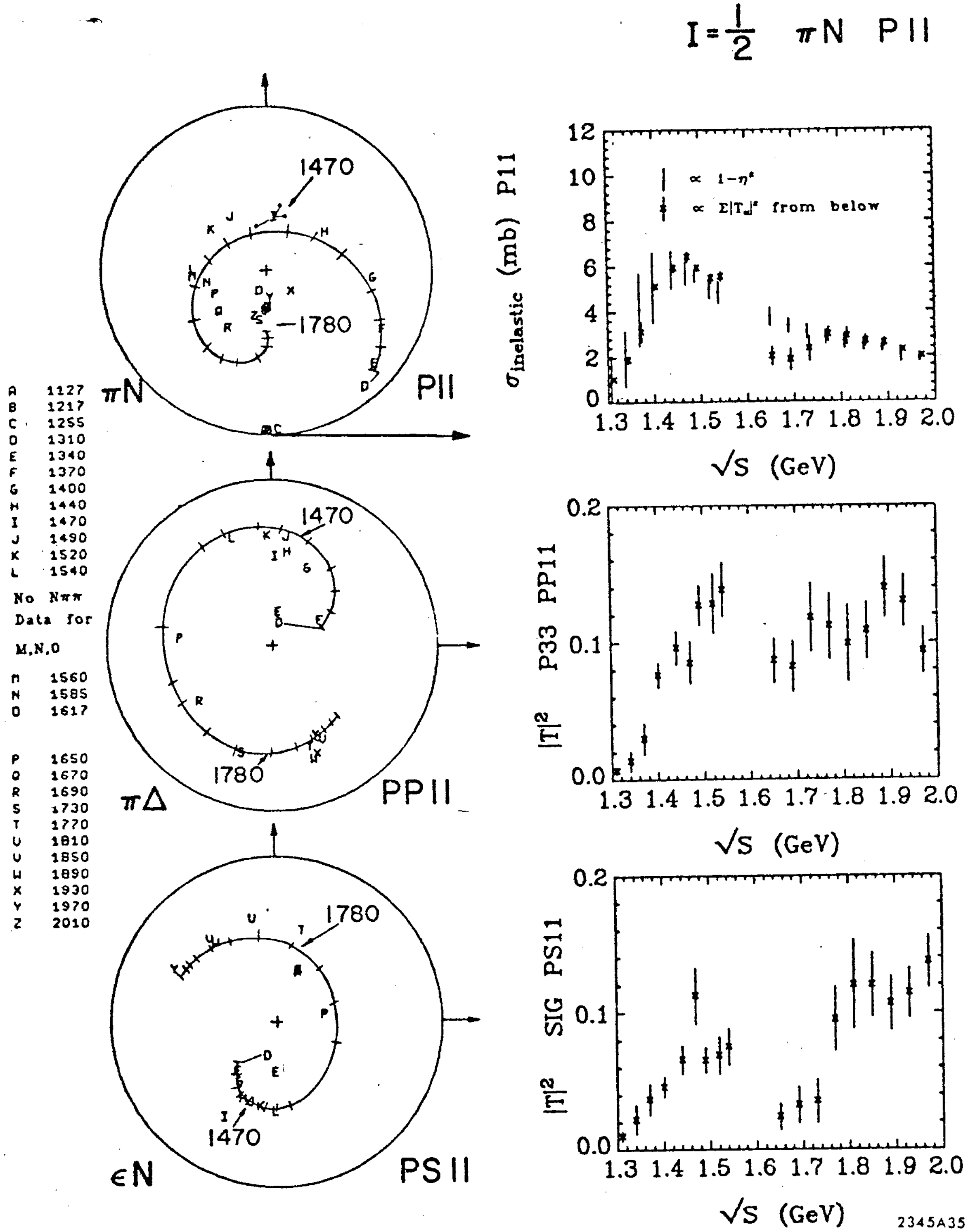

I = 1/2 πN P11
1470
1780
πN
P11
A 1127
B 1217
C 1255
D 1310
E 1340
F 1370
G 1400
H 1440
I 1470
J 1490
K 1520
L 1540
No Nππ
Data for
M,N,O
M 1560
N 1585
O 1617
P 1650
Q 1670
R 1690
S 1730
T 1770
U 1810
V 1850
W 1890
X 1930
Y 1970
Z 2010
πΔ
PP11
εN
PS11
σ inelastic (mb) P11
∝ 1−η²
∝ Σ|T_J|² from below
√s (GeV)
|T|² P33 PP11
|T|² SIG PS11
2345A35

Fig. 4

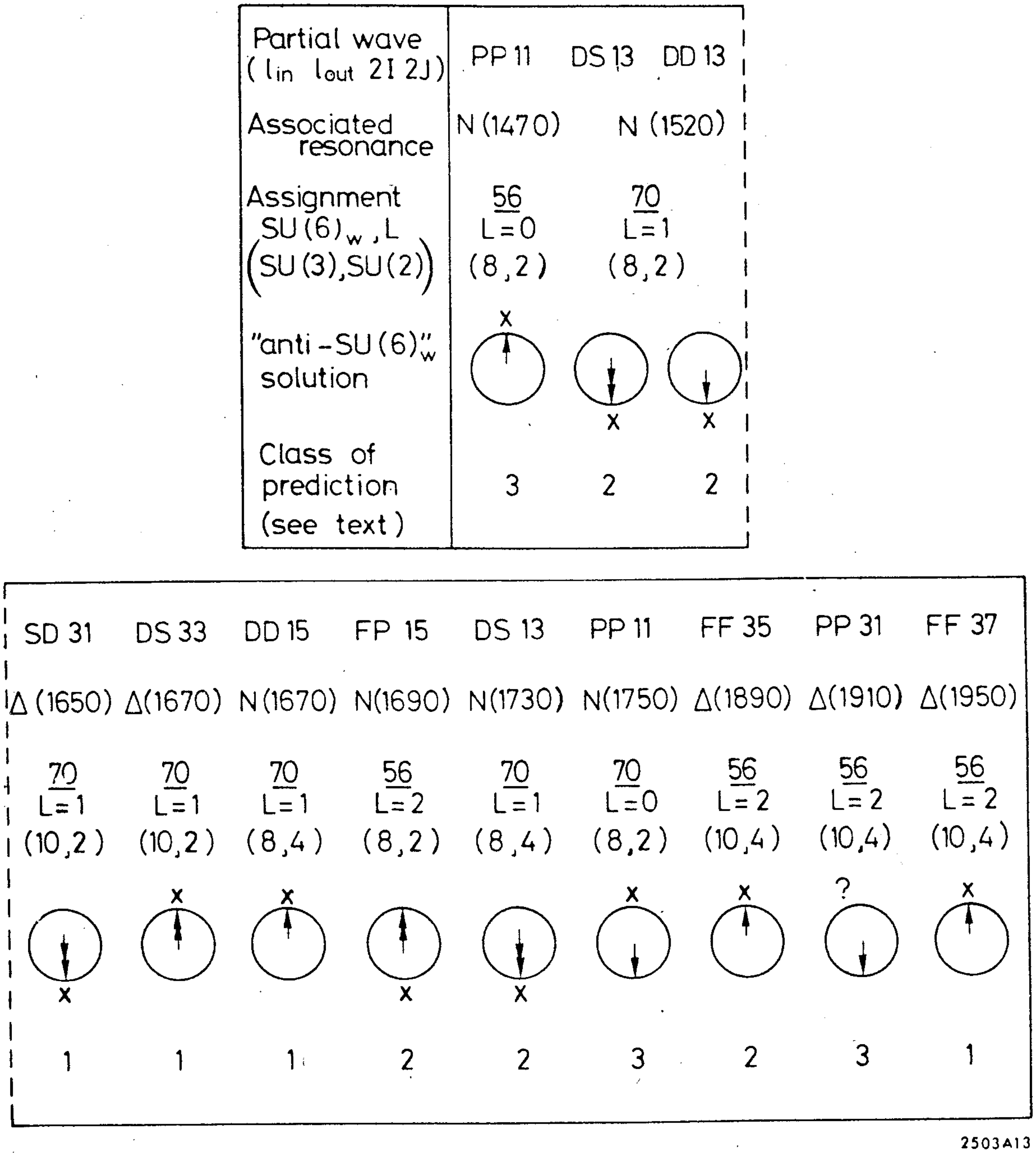
Partial wave (l_{in} l_{out} 2I 2J)
PP 11 DS 13 DD 13
Associated resonance
N (1470) N (1520)
Assignment SU(6)$_w$, L (SU(3), SU(2))
56 L=0 (8,2)
70 L=1 (8,2)
"anti-SU(6)$_w$" solution
x x x
Class of prediction (see text)
3 2 2
SD 31 DS 33 DD 15 FP 15 DS 13 PP 11 FF 35 PP 31 FF 37
Δ(1650) Δ(1670) N(1670) N(1690) N(1730) N(1750) Δ(1890) Δ(1910) Δ(1950)
70 L=1 (10,2)
70 L=1 (10,2)
70 L=1 (8,4)
56 L=2 (8,2)
70 L=1 (8,4)
70 L=0 (8,2)
56 L=2 (10,4)
56 L=2 (10,4)
56 L=2 (10,4)
x x x x x x x x ?
1 1 1 2 2 3 2 3 1
2503A13

Fig. 5

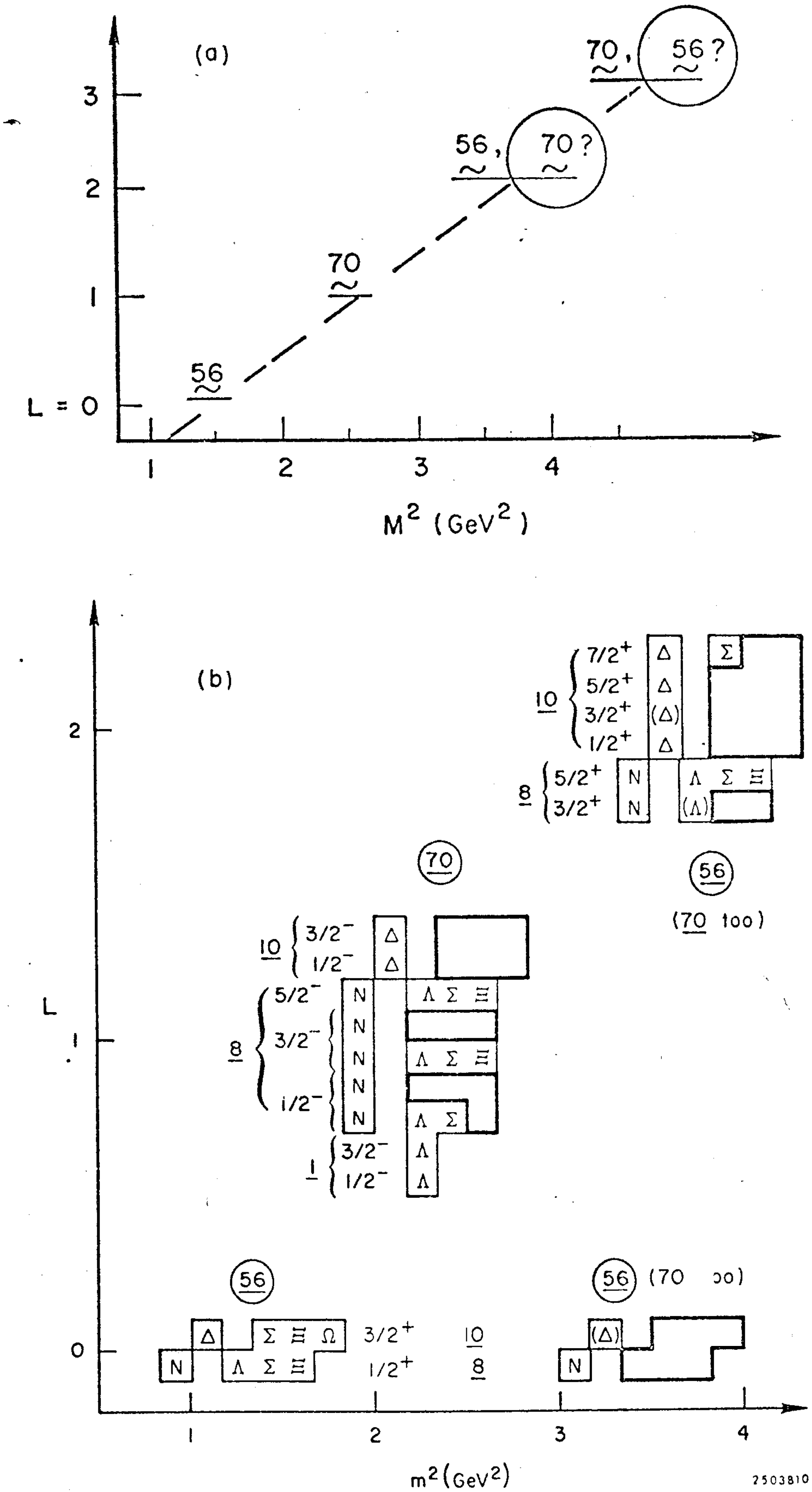

Fig. 6

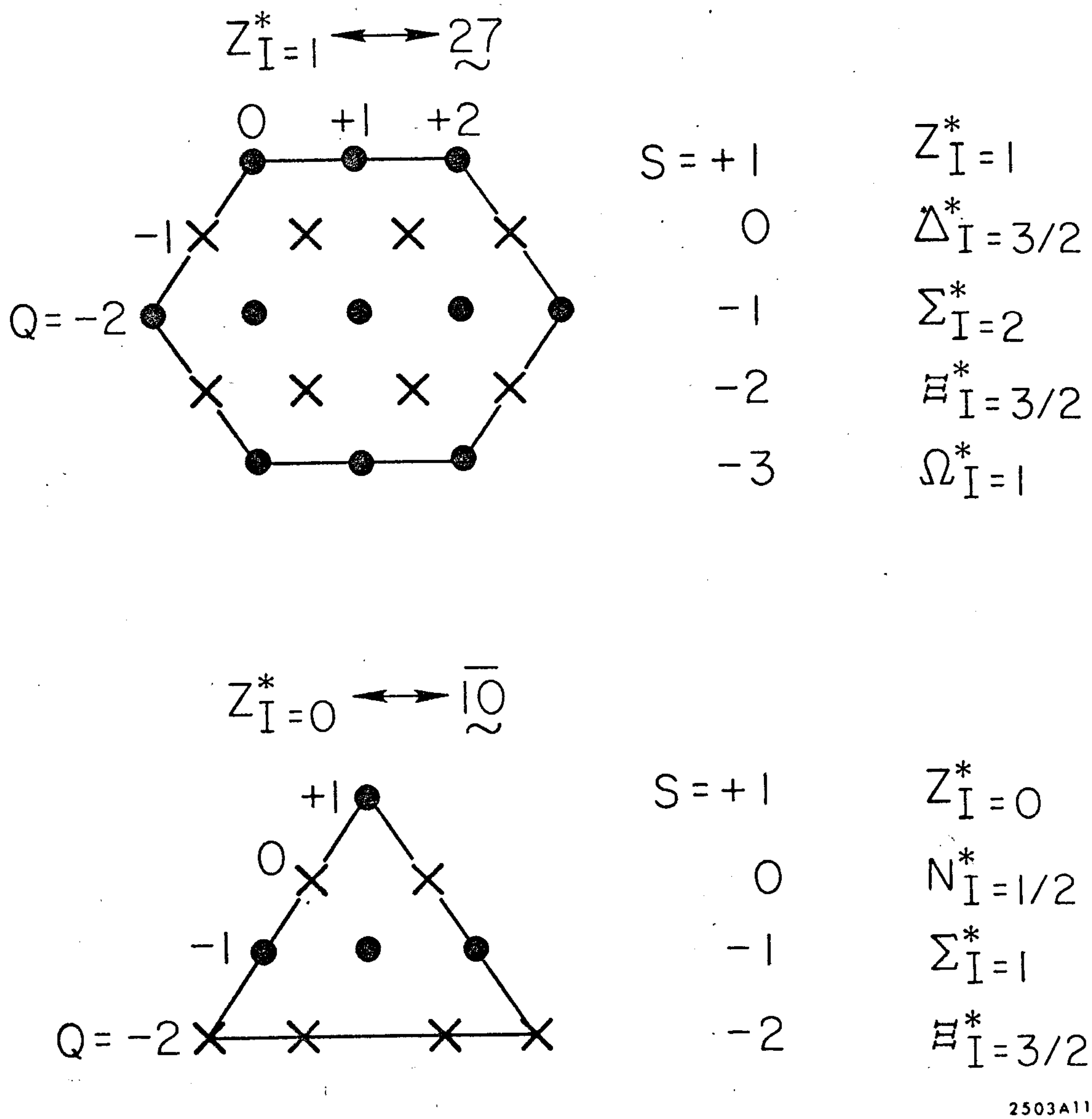

$Z^*_{I=1} \longleftrightarrow \underset{\sim}{27}$
0 +1 +2
−1
Q = −2
S = +1 $Z^*_{I=1}$
0 $\Delta^*_{I=3/2}$
−1 $\Sigma^*_{I=2}$
−2 $\Xi^*_{I=3/2}$
−3 $\Omega^*_{I=1}$
$Z^*_{I=0} \longleftrightarrow \underset{\sim}{\overline{10}}$
+1
0
−1
Q = −2
S = +1 $Z^*_{I=0}$
0 $N^*_{I=1/2}$
−1 $\Sigma^*_{I=1}$
−2 $\Xi^*_{I=3/2}$
2503A11

Fig. 7

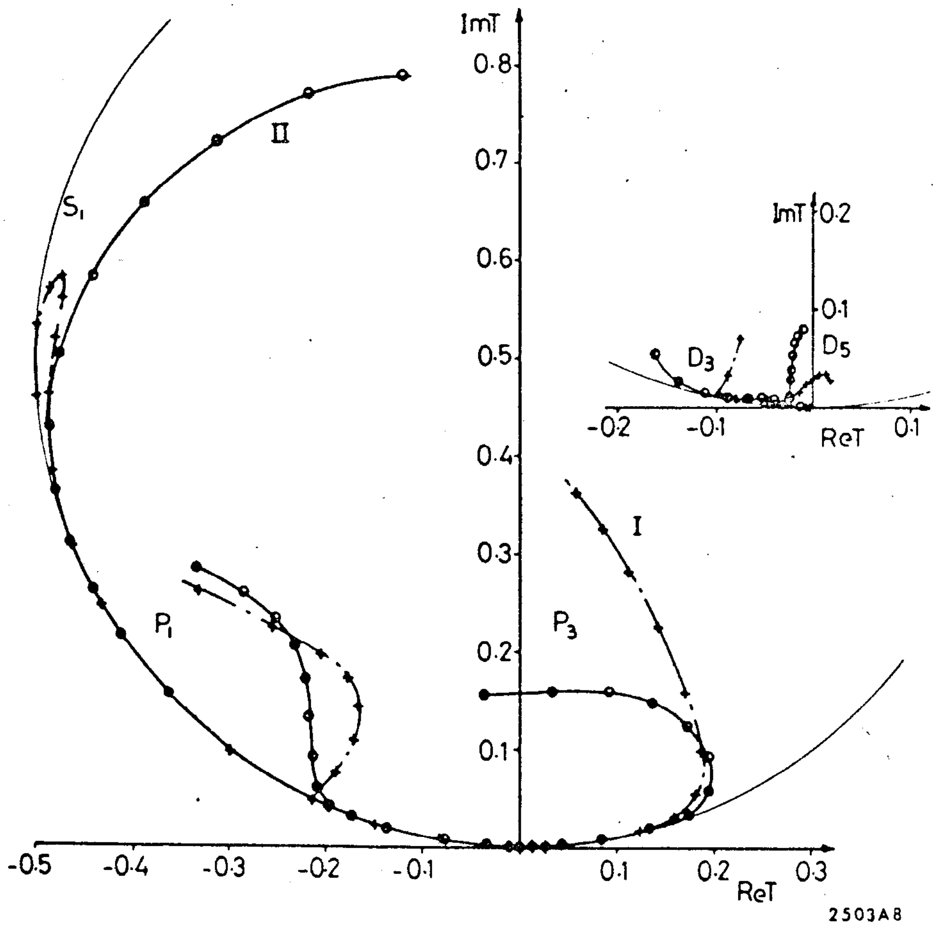

ImT
0.8
0.7
0.6
0.5
0.4
0.3
0.2
0.1
II
S1
P1
P3
I
ImT 0.2
0.1
D3
D5
-0.2
-0.1
0.1
ReT
-0.5
-0.4
-0.3
-0.2
-0.1
0.1
0.2
0.3
ReT
2503A8

Fig. 8

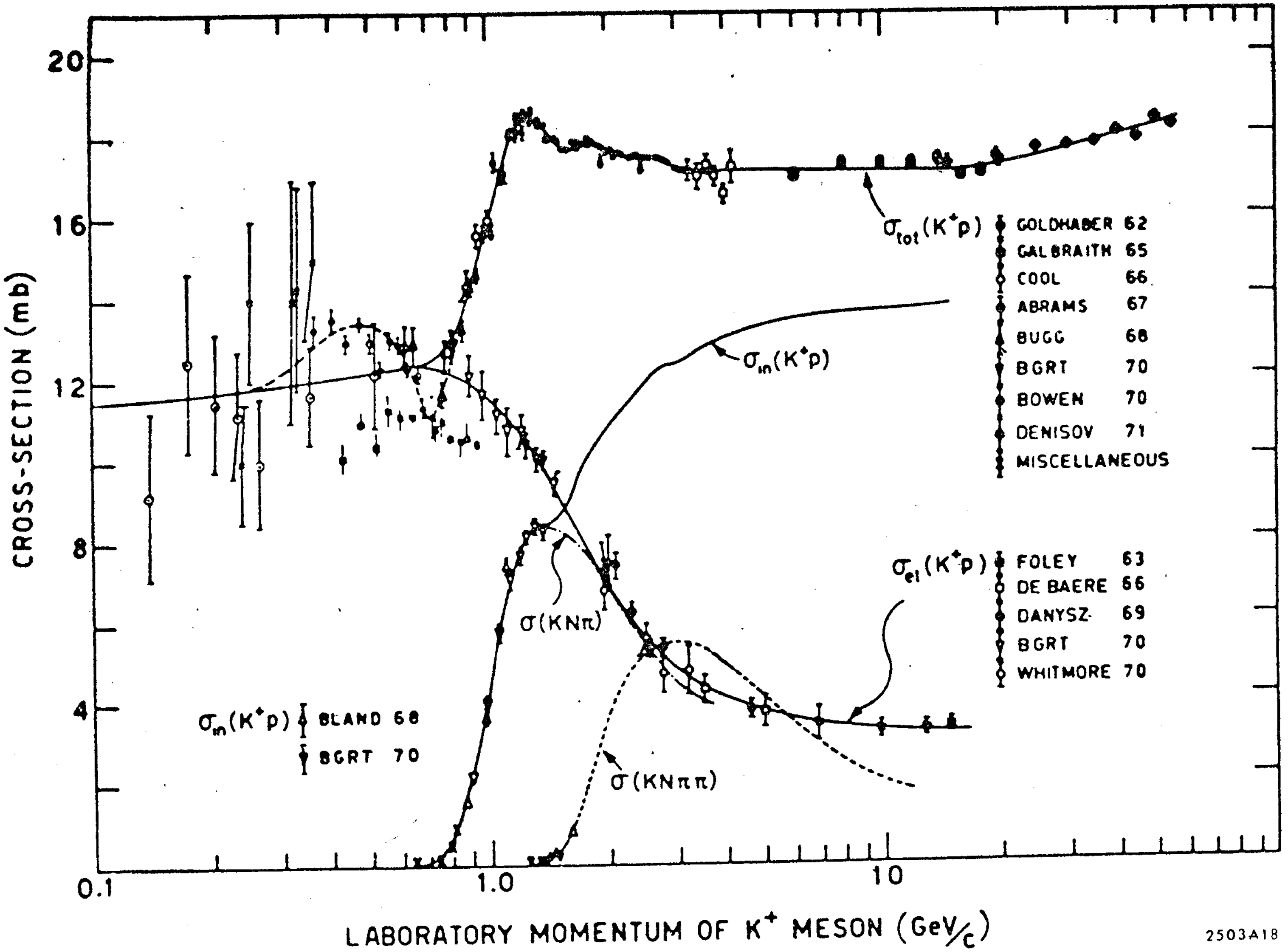

20
16
12
8
4
CROSS-SECTION (mb)
0.1
1.0
10
LABORATORY MOMENTUM OF K⁺ MESON (GeV/c)
2503A18
σ_tot(K⁺p)
GOLDHABER 62
GALBRAITH 65
COOL 66
ABRAMS 67
BUGG 68
BGRT 70
BOWEN 70
DENISOV 71
MISCELLANEOUS
σ_in(K⁺p)
σ(KNπ)
σ_el(K⁺p)
FOLEY 63
DE BAERE 66
DANYSZ 69
BGRT 70
WHITMORE 70
σ_in(K⁺p)
BLAND 68
BGRT 70
σ(KNππ)

Fig. 9

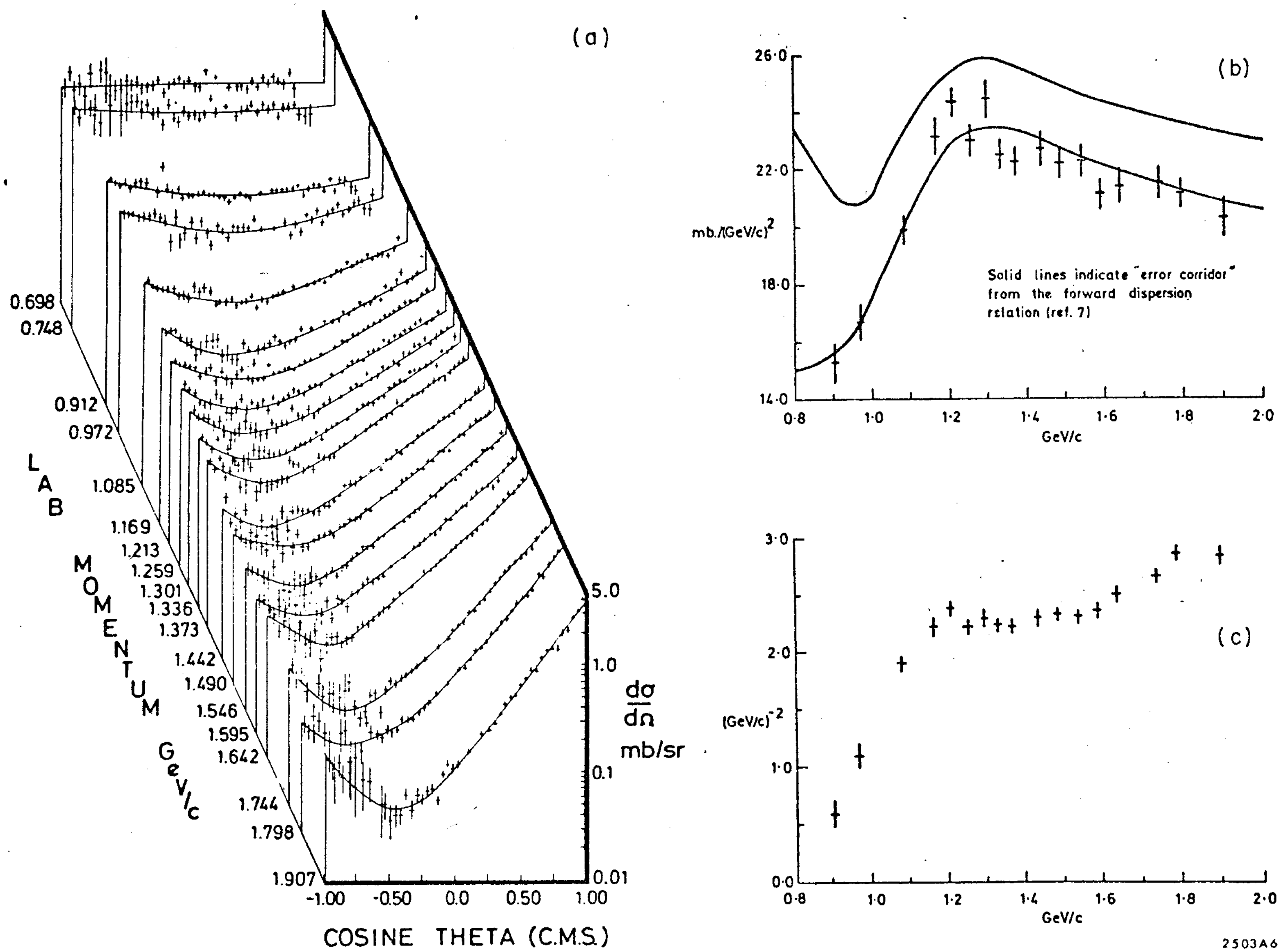
(a)
LAB MOMENTUM GeV/c
0.698
0.748
0.912
0.972
1.085
1.169
1.213
1.259
1.301
1.336
1.373
1.442
1.490
1.546
1.595
1.642
1.744
1.798
1.907
5.0
1.0
0.1
0.01
dσ/dΩ mb/sr
-1.00
-0.50
0.0
0.50
1.00
COSINE THETA (C.M.S.)
(b)
26·0
22·0
18·0
14·0
mb./(GeV/c)²
Solid lines indicate "error corridor" from the forward dispersion relation (ref. 7)
0·8
1·0
1·2
1·4
1·6
1·8
2·0
GeV/c
(c)
3·0
2·0
1·0
0·0
(GeV/c)⁻²
0·8
1·0
1·2
1·4
1·6
1·8
2·0
GeV/c
2503A6

Fig. 10

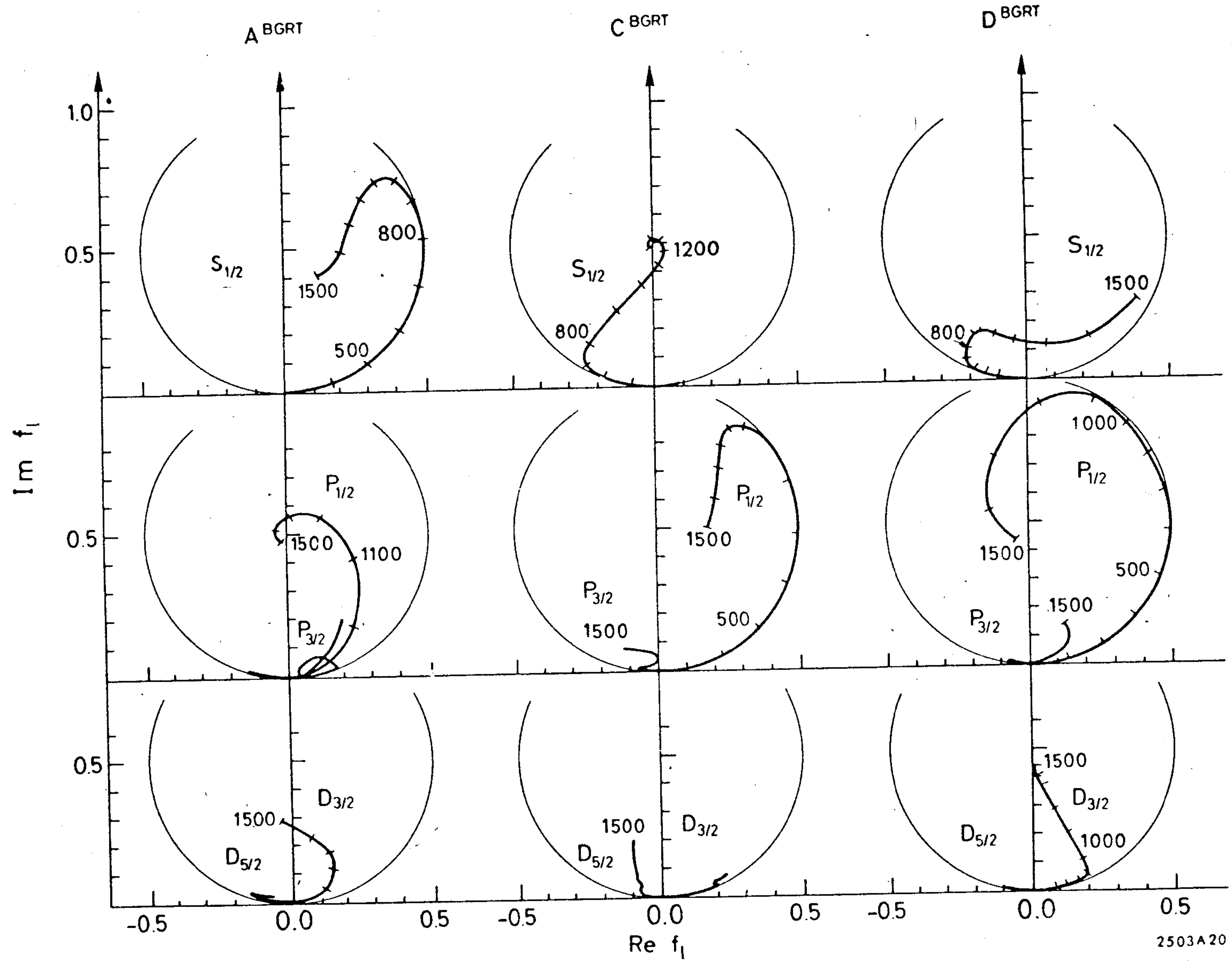

A^{BGRT}
C^{BGRT}
D^{BGRT}
1.0
0.5
0.5
0.5
Im f_l
$S_{1/2}$
800
1500
500
1200
800
1500
$P_{1/2}$
1500
1100
$P_{3/2}$
500
1000
$D_{3/2}$
$D_{5/2}$
-0.5
0.0
0.5
Re f_l
2503A20

Fig. 11

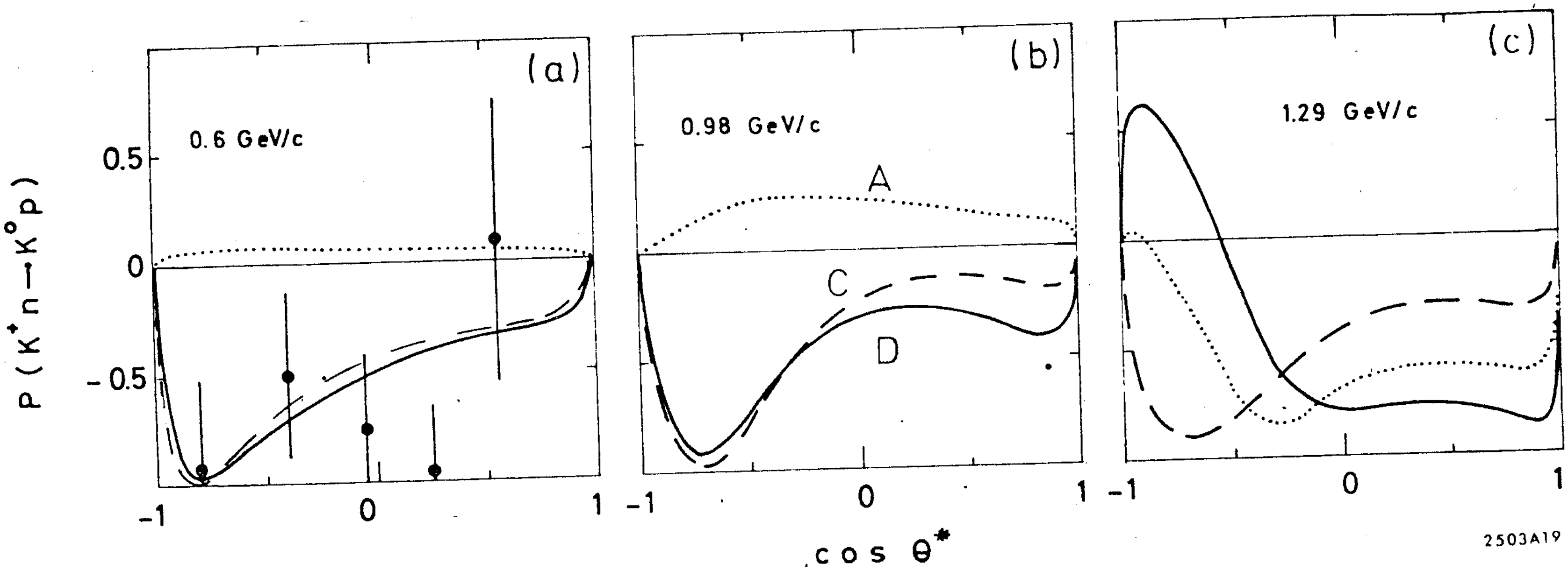
(a)
0.6 GeV/c
0.5
0
- 0.5
-1
0
1
P (K⁺n ⟶ K°p)
(b)
0.98 GeV/c
A
C
D
-1
0
1
cos θ*
(c)
1.29 GeV/c
-1
0
1
2503A19

Fig. 12a

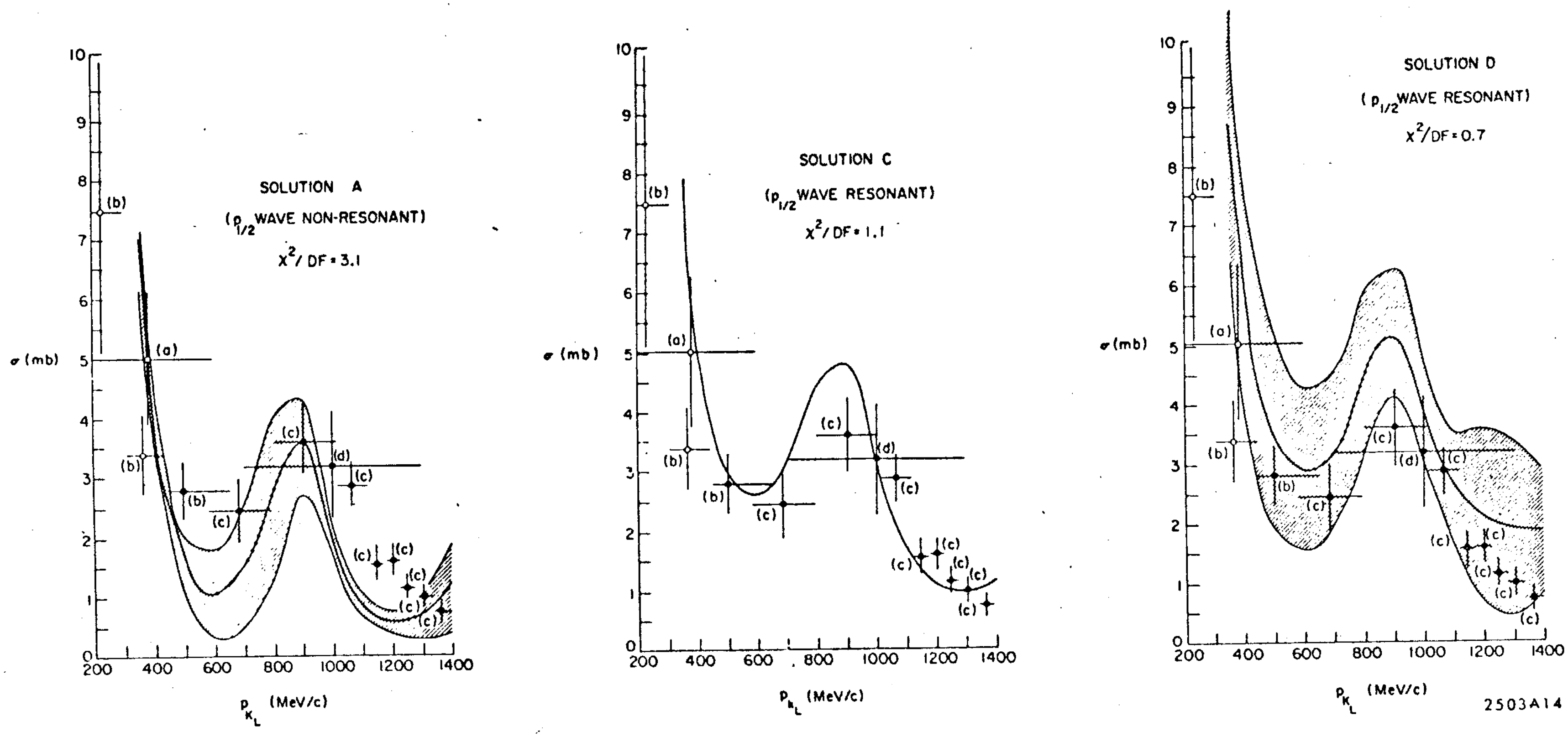

SOLUTION A
($p_{1/2}$ WAVE NON-RESONANT)
χ^2/ DF = 3.1
σ (mb)
p_{K_L} (MeV/c)
SOLUTION C
($p_{1/2}$ WAVE RESONANT)
χ^2/ DF = 1.1
σ (mb)
p_{K_L} (MeV/c)
SOLUTION D
($p_{1/2}$ WAVE RESONANT)
χ^2/DF = 0.7
σ (mb)
p_{K_L} (MeV/c)
2503A14

Fig. 12b

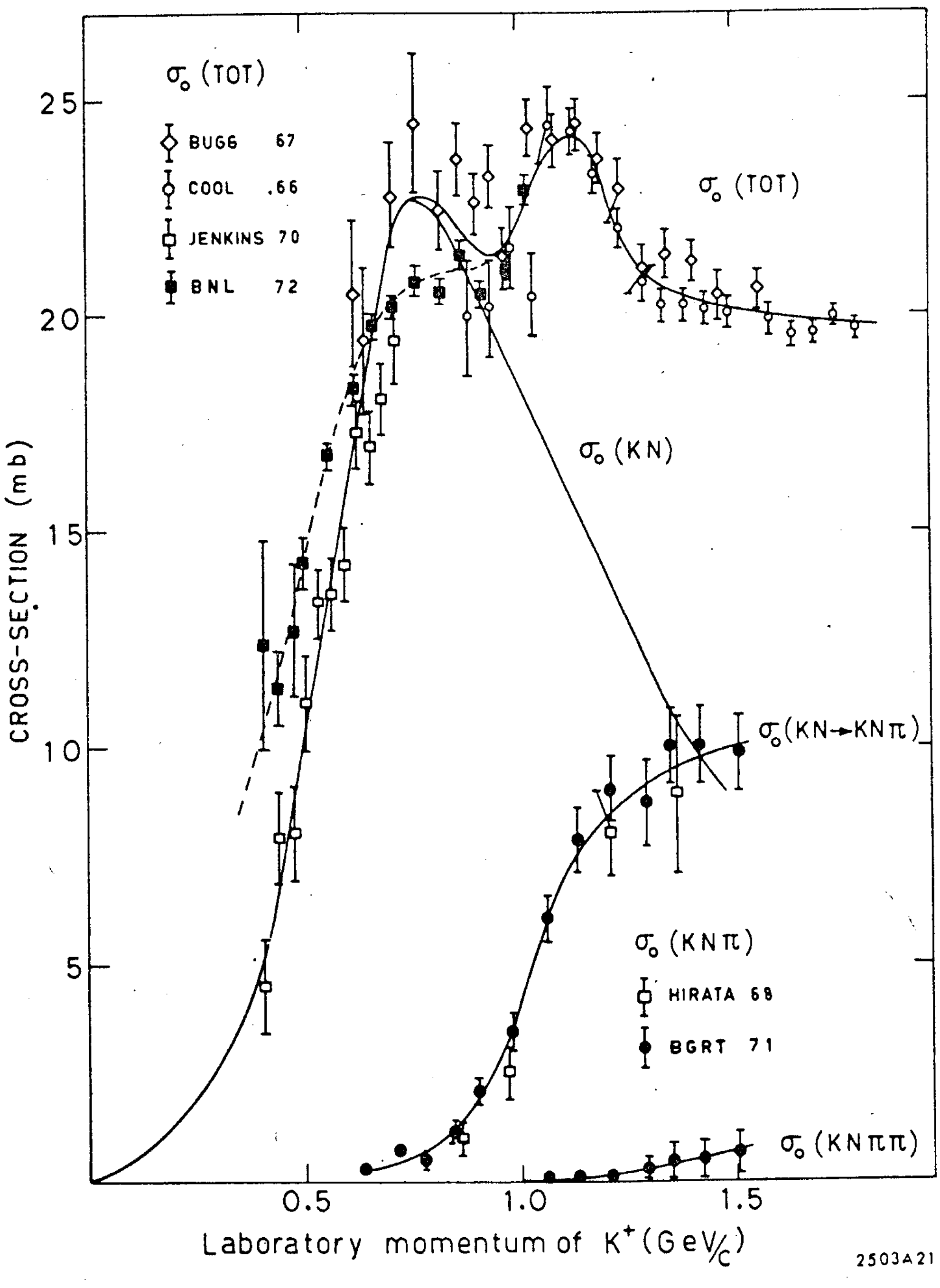

σ₀ (TOT)
BUGG 67
COOL 66
JENKINS 70
BNL 72
σ₀ (TOT)
σ₀ (KN)
σ₀(KN→KNπ)
σ₀ (KNπ)
HIRATA 68
BGRT 71
σ₀ (KNππ)
25
20
15
10
5
0.5
1.0
1.5
CROSS-SECTION (mb)
Laboratory momentum of K⁺ (GeV/c)
2503A21

Fig. 13

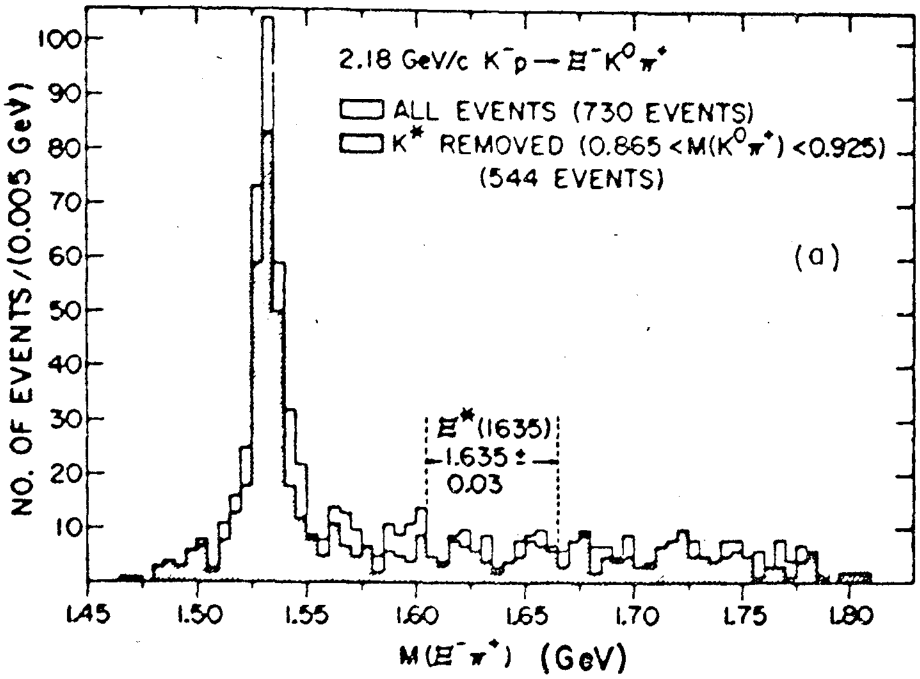

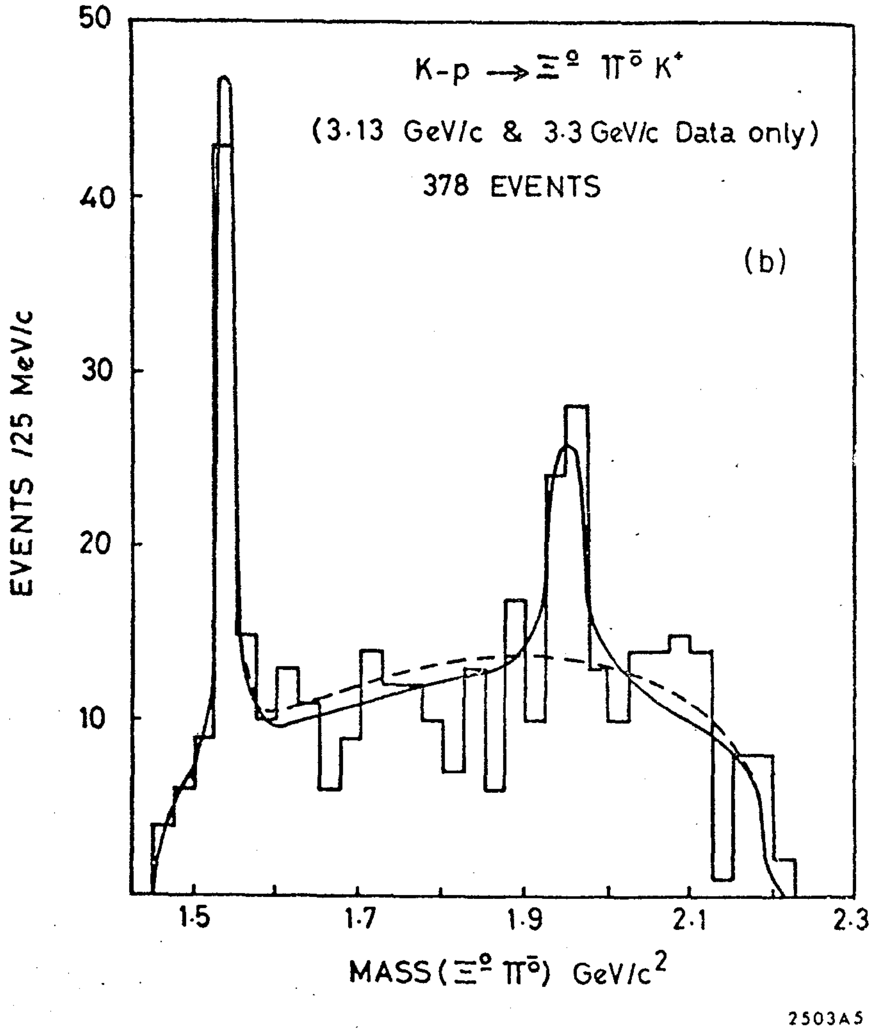

2503A5

Fig. 14

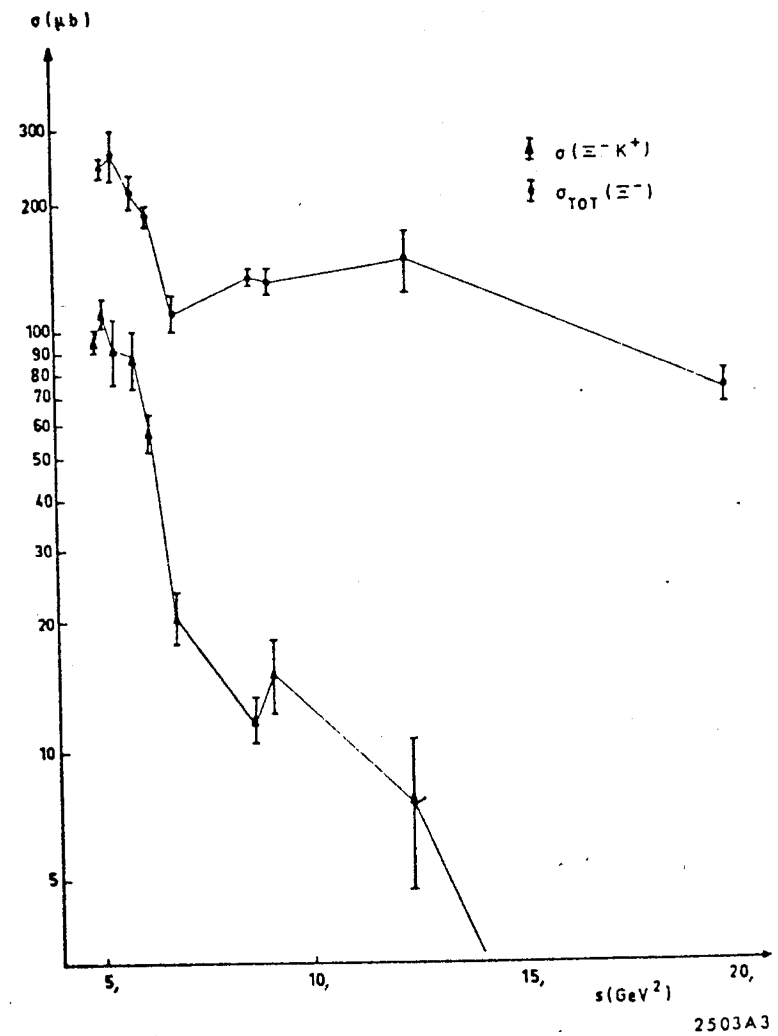

σ(μb)
300
200
100
90
80
70
60
50
40
30
20
10
5
σ(Ξ⁻K⁺)
σ_TOT(Ξ⁻)
5,
10,
15,
20,
s(GeV²)
2503A3

Fig. 15

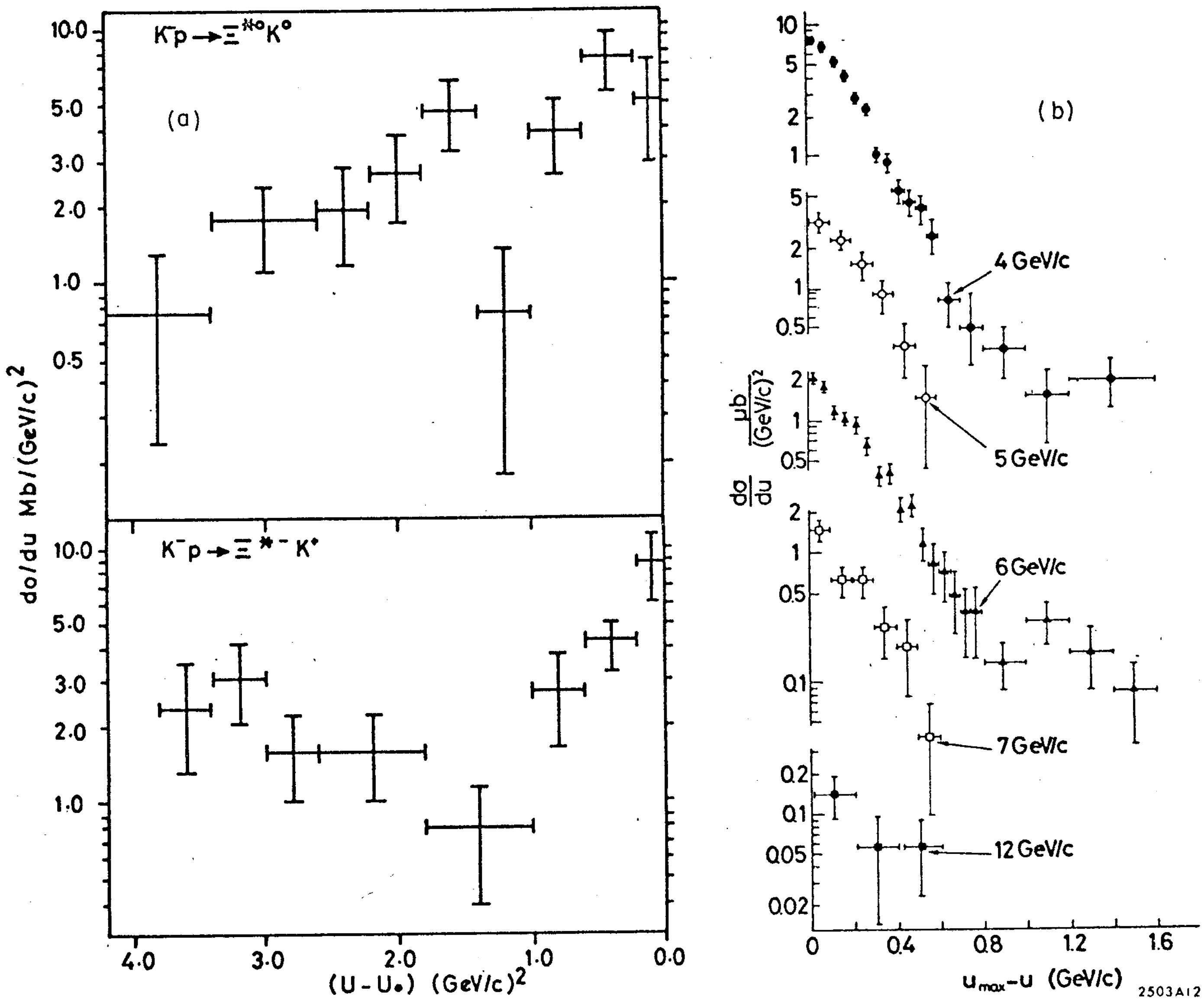

K⁻p → Ξ*⁰K⁰
(a)
K⁻p → Ξ*⁻K⁺
dσ/du Mb/(GeV/c)²
(U - U₀) (GeV/c)²
(b)
4 GeV/c
5 GeV/c
6 GeV/c
7 GeV/c
12 GeV/c
dσ/du μb/(GeV/c)²
u_max - u (GeV/c)
2503A12

Fig. 16

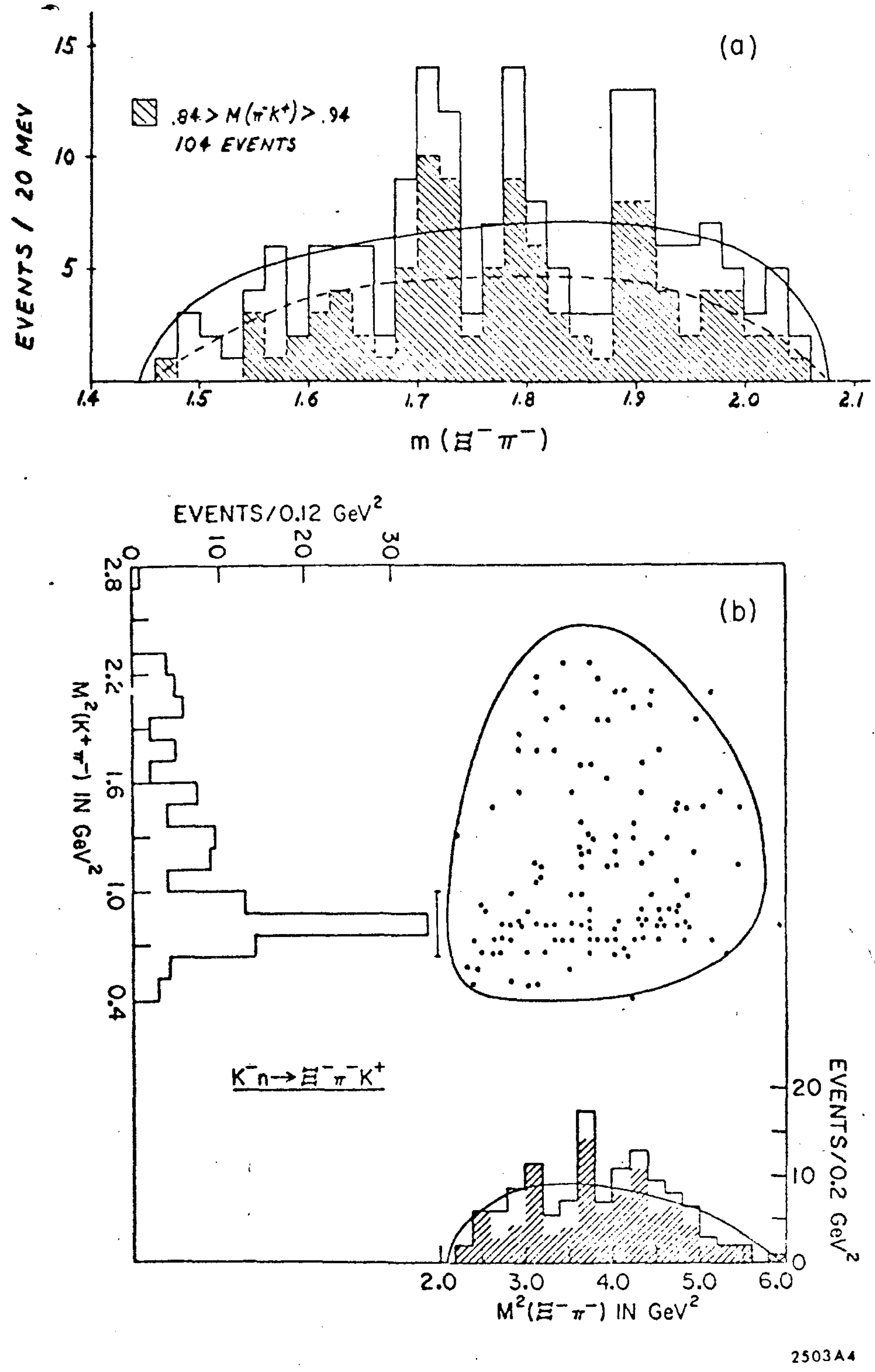

(a)
.84 > M(π⁻K⁺) > .94
104 EVENTS
EVENTS / 20 MEV
m (Ξ⁻π⁻)
(b)
EVENTS/0.12 GeV²
M²(K⁺π⁻) IN GeV²
K⁻n→Ξ⁻π⁻K⁺
EVENTS/0.2 GeV²
M²(Ξ⁻π⁻) IN GeV²
2503A4

Fig. 17

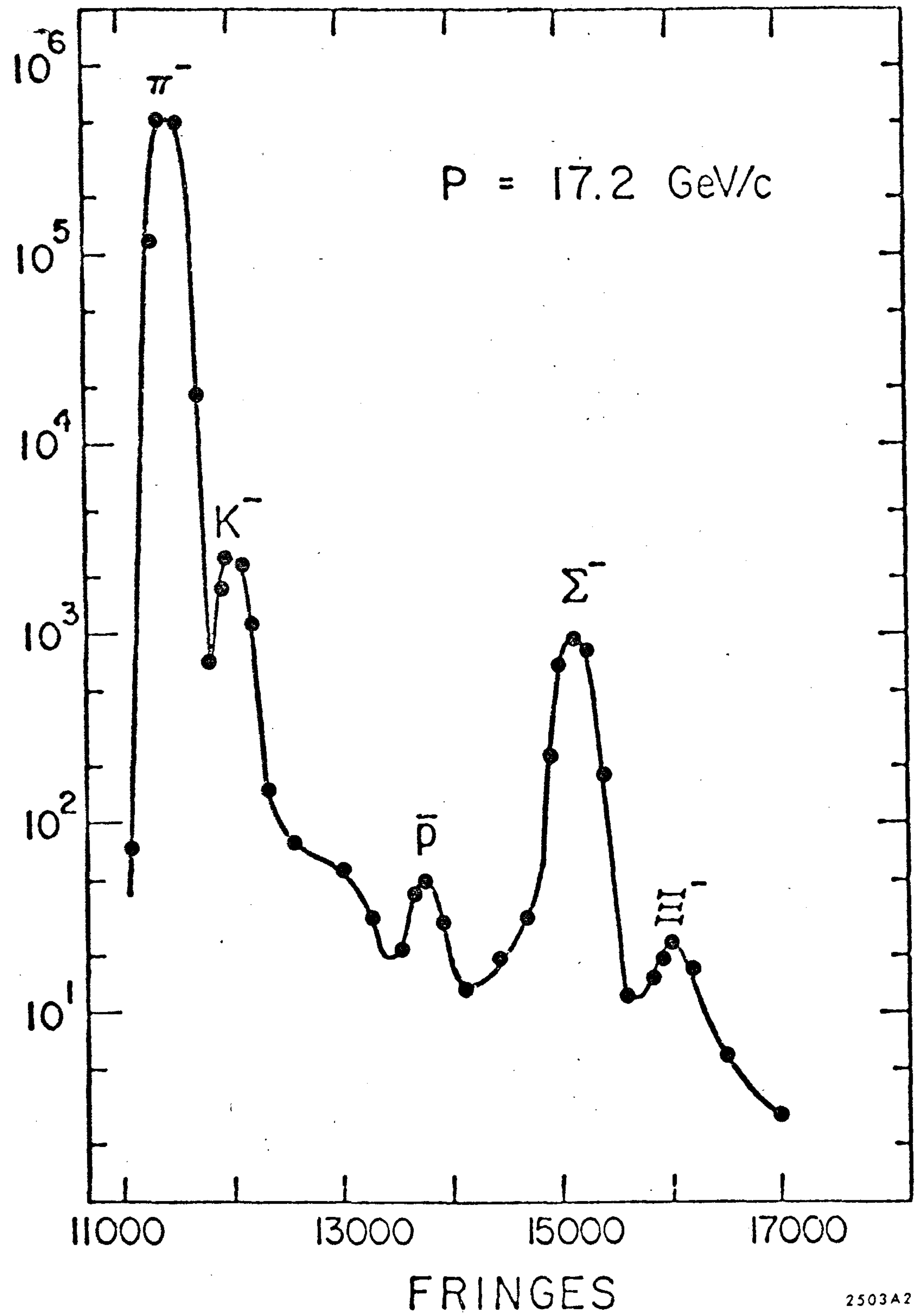

10^6
10^5
10^4
10^3
10^2
10^1
π^-
K^-
$\bar{p}$
Σ^-
Ξ^-
P = 17.2 GeV/c
11000
13000
15000
17000
FRINGES
2503A2

Fig. 18

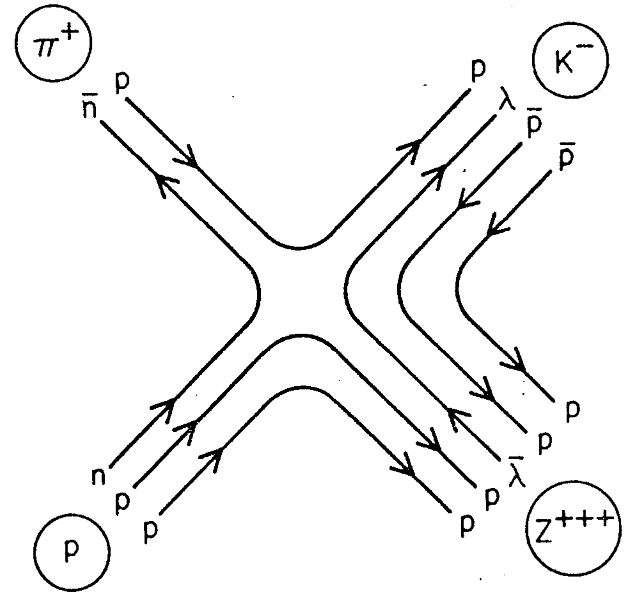

(a)

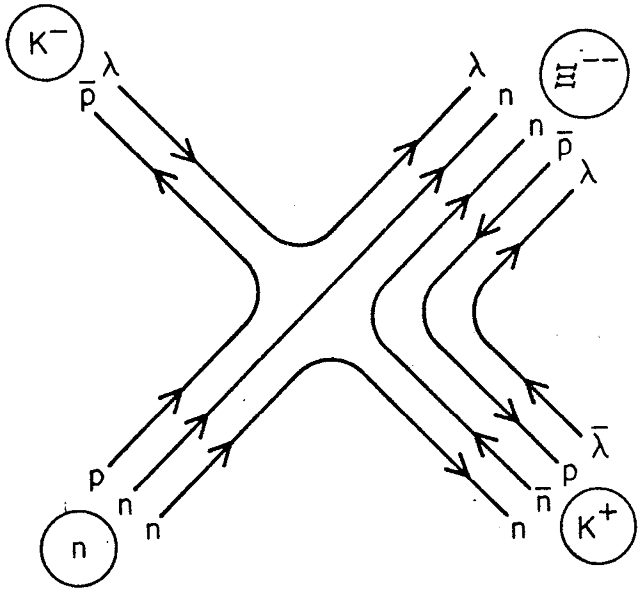

(b)

2503A1

Fig. 19

CERN

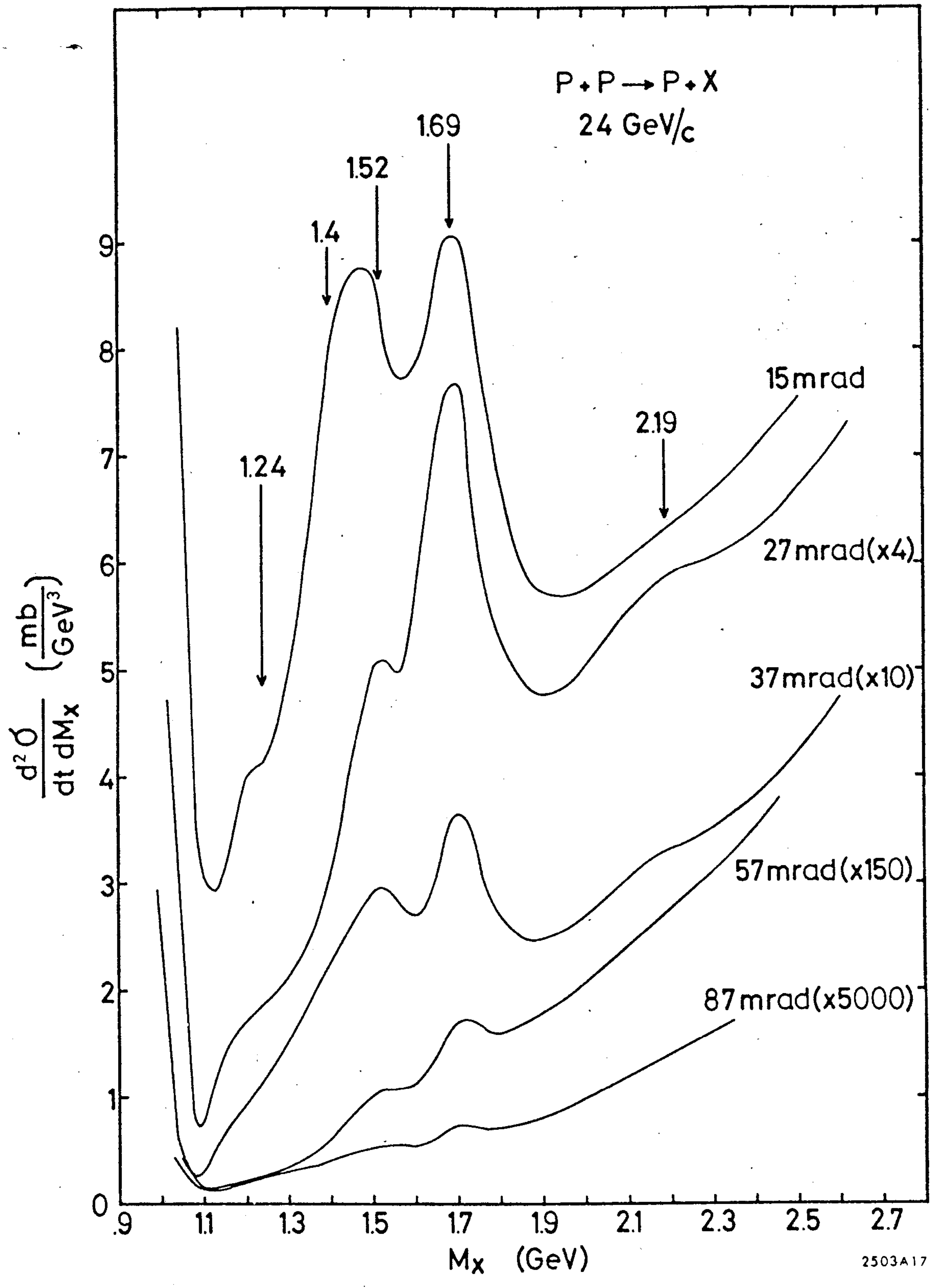

P + P → P + X
24 GeV/c
1.69
1.52
1.4
1.24
2.19
15 mrad
27 mrad(x4)
37 mrad(x10)
57 mrad(x150)
87 mrad(x5000)
$\frac{d^2\sigma}{dt\,dM_X}$ $\left(\frac{mb}{GeV^3}\right)$
0
1
2
3
4
5
6
7
8
9
.9
1.1
1.3
1.5
1.7
1.9
2.1
2.3
2.5
2.7
M_X (GeV)
2503A17

Fig. 20

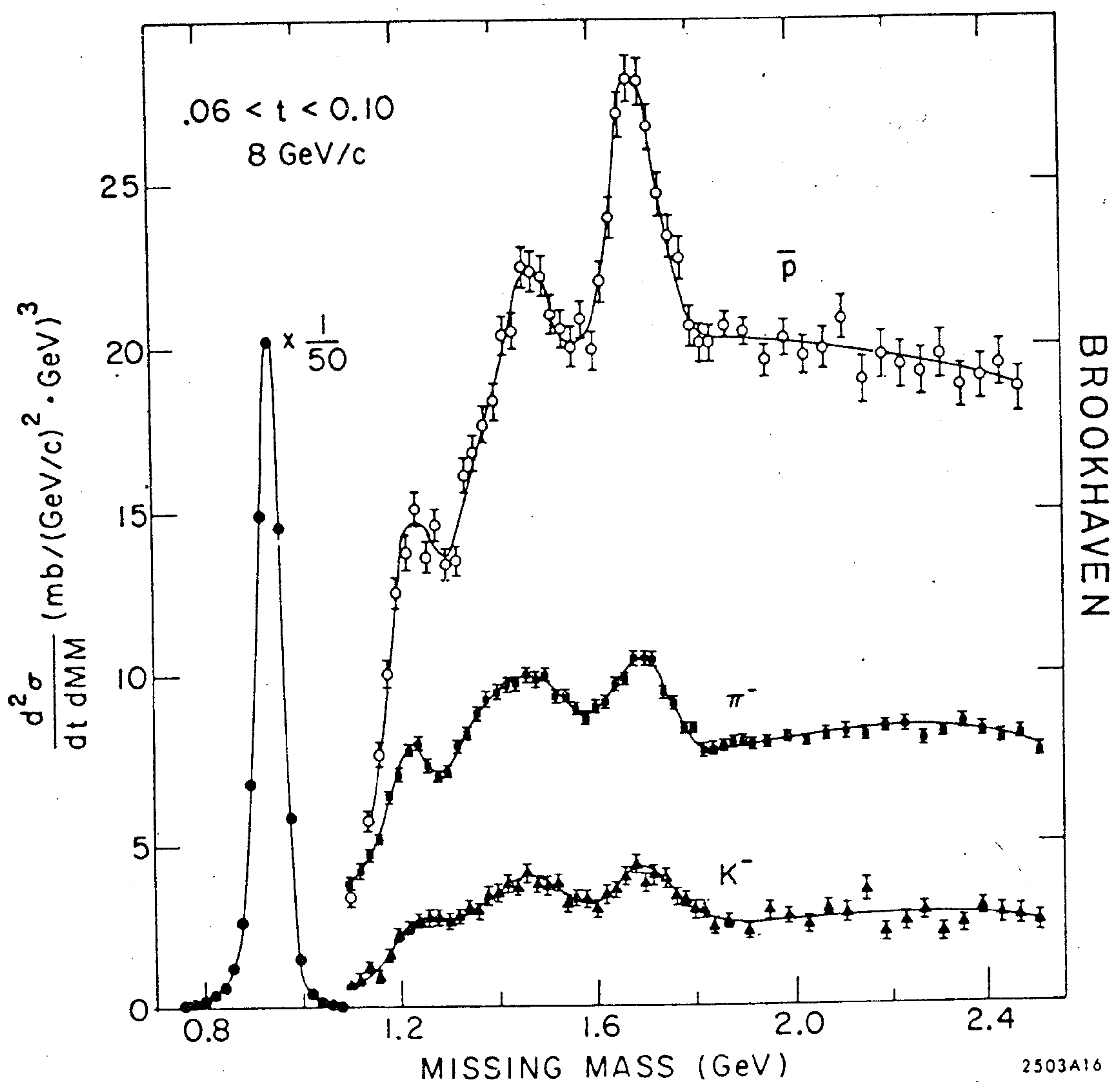
.06 < t < 0.10
8 GeV/c
× 1/50
$\bar{p}$
π^-
K^-
BROOKHAVEN
$\frac{d^2\sigma}{dt\,dMM}$ (mb/(GeV/c)^2 · GeV)^3
MISSING MASS (GeV)
0
5
10
15
20
25
0.8
1.2
1.6
2.0
2.4
2503A16

Fig. 21

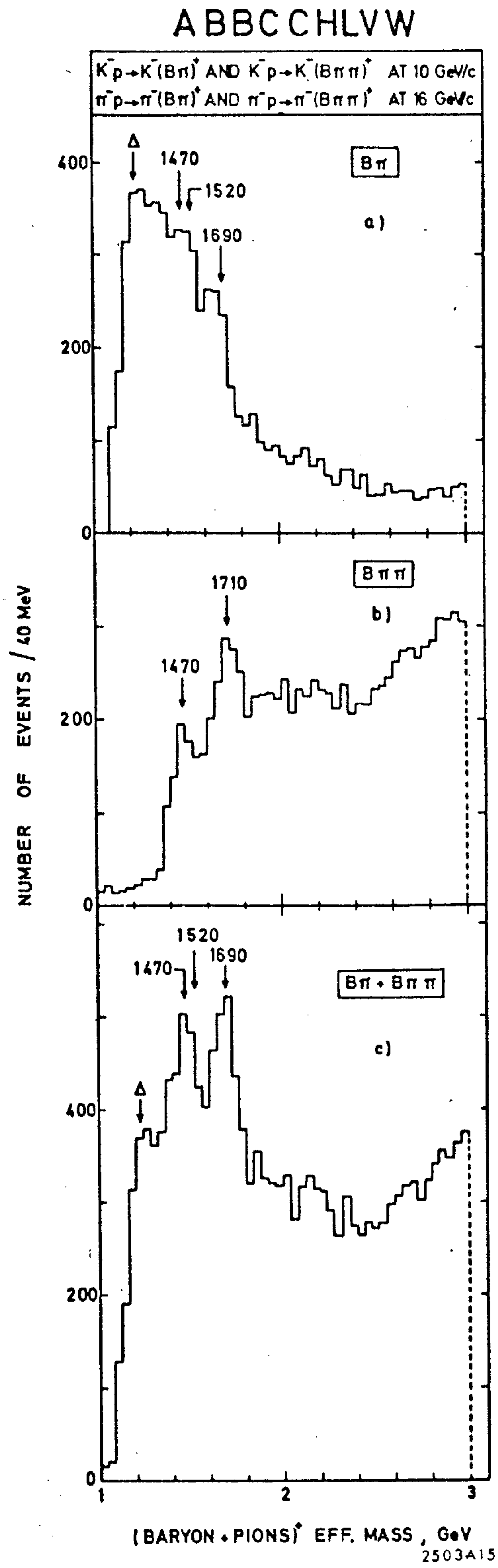
ABBCCHLVW
$K^-p \to K^-(B\pi)^+$ AND $K^-p \to K^-(B\pi\pi)^+$ AT 10 GeV/c
$\pi^-p \to \pi^-(B\pi)^+$ AND $\pi^-p \to \pi^-(B\pi\pi)^+$ AT 16 GeV/c
Bπ
a)
Δ
1470
1520
1690
Bππ
b)
1710
1470
Bπ + Bππ
c)
1520
1470
1690
Δ
NUMBER OF EVENTS / 40 MeV
(BARYON + PIONS)$^+$ EFF. MASS, GeV
2503A15

Fig. 22